

# The high temperature phase transition for $\phi^4$ theories

N. Tetradis and C. Wetterich

*Deutsches Elektronen-Synchrotron DESY, W-2000 Hamburg 52, FRG*

Received 6 July 1992

(Revised 25 September 1992)

Accepted for publication 10 February 1993

We investigate the temperature dependent effective potential for  $N$ -component  $\phi^4$  theories with a new method based on averages of fields. The effective three-dimensional running of couplings at scales much below the temperature is described. We obtain a detailed quantitative picture of the second order phase transition, including the critical exponents for the behaviour in the vicinity of the critical temperature.

## 1. Introduction

Spontaneous symmetry breaking is one of the most prominent features of the standard model of electroweak interactions. The masses of the gauge bosons and fermions are proportional to the vacuum expectation value  $\rho_0^{1/2} = 174$  GeV of the Higgs doublet  $\phi$ . The Fermi scale  $\rho_0^{1/2}$  is a constant only in the vacuum, while in a thermal equilibrium state it depends on the temperature. At temperature much higher than  $\rho_0^{1/2}$  the symmetry is restored and  $\rho_0(T)$  vanishes [1–3]. Such high temperatures were presumably realized in the very early universe immediately after the big bang. As the universe cooled there must have been a phase transition from the symmetric to the spontaneously broken phase of the standard model. This phase transition may have many important consequences for our present universe. One example is the possible creation of the excess of matter compared to antimatter (baryon asymmetry) during this transition [4,5].

The physical implications of the high temperature electroweak phase transition are quite different if it is second order or first order. This question has not yet been settled in the context of the high temperature perturbation theory [2] since these calculations are affected by severe infrared problems [1,3,6]. For a very small Higgs mass or, equivalently, for a small ratio between the quartic scalar coupling  $\lambda$  and the gauge coupling squared  $g^2$ , one expects the transition to be first order. This follows from continuity arguments if the Coleman–Weinberg symmetry breaking [7] gives a qualitatively correct picture at vanishing temperature. For realistic values of  $\lambda/g^2$  of order one or larger the issue becomes more

involved. It has been argued [8] that the fluctuations of the gauge bosons induce a non-analytic term  $\sim T(\phi^\dagger\phi)^{3/2}$  in the effective potential for the scalar field  $\phi$  at non-vanishing temperature. The existence of such a term for  $\phi \rightarrow 0$  would necessarily imply a first order phase transition. In high temperature perturbation theory the one loop contribution to the quartic scalar coupling induces a term in the temperature dependent effective potential

$$\sim g^4 \frac{T}{k} (\phi^\dagger\phi)^2, \quad (1.1)$$

where  $k$  is an appropriate infrared cutoff. In the symmetric phase ( $\phi = 0$ ) the gauge bosons are massless and (1.1) is infrared divergent for  $k \rightarrow 0$  (unless regulated by an effective “magnetic mass”). In the spontaneously broken phase the gauge bosons acquire a mass  $\sim g\phi$ . This acts as an infrared regulator, i.e.  $k^2 \sim g^2(\phi^\dagger\phi)$ . Inserting this expression into (1.1) induces the non-analytic behaviour alluded to above. Nevertheless, the existence of this “cubic term” for  $\phi \rightarrow 0$  remains highly questionable since the same sort of infrared divergences also appear in the computation of the effective temperature dependent gauge coupling  $g$ . This effect is not accounted for in the usual treatment, where  $g$  is taken independent of  $k$  in (1.1). A proper renormalization of  $g$  may alter the reasoning leading to the “cubic term” for  $\phi \rightarrow 0$ .

The inclusion of scalar fluctuations in the high temperature expansion is even more problematic, since infrared divergences from the massless scalar fluctuations appear also for non-vanishing  $\phi$  (at the turning point between the minimum of the potential at  $\phi_0 \neq 0$  and the maximum). The scalar one loop contribution to the potential contains a term analogous to (1.1), i.e.

$$\sim \lambda^2 \frac{T}{k} (\phi^\dagger\phi)^2. \quad (1.2)$$

If one identifies  $k^2$  with the effective temperature dependent mass term for the radial mode for  $\phi \neq 0$ , i.e.  $m^2(T) + 3\lambda(\phi^\dagger\phi)$ , one may again conclude that there is a non-analytic “cubic term” for the temperature at which  $m^2(T)$  vanishes. This has led some authors to speculate [9] that the high temperature phase transition may be first order even in a pure scalar theory. Most evidence indicates, however, that  $N$ -component  $\phi^4$  theories exhibit a second order phase transition. Again, the problem comes from the use of a constant  $\lambda$  in (1.2). This neglects the running of  $\lambda$  as a function of  $k$ . Shortly speaking, it is not consistent to include for  $T \gg k$  the strong renormalization effects of the quartic coupling in the effective potential (1.2), but to neglect the same effect for the running of  $\lambda$  itself.

The strong infrared effects discussed above result from the three-dimensional character of the effective theory for the modes with momenta much smaller than  $T$ . The effective three-dimensional quartic coupling is  $\lambda T$  and has the dimension of mass. In consequence, the running as a function of the infrared

cutoff  $k$  is very different from the logarithmic four-dimensional running. At the phase transition one expects for  $k \rightarrow 0$  an infrared stable fixed point for the ratio  $\lambda(k, T)T/k$ . Then  $\lambda(k, T)$  vanishes  $\sim k$  and the infrared divergence in the quartic term (1.2) disappears. For a correct description of the phase transition one needs suitable infrared evolution equations which describe the dependence of  $\lambda$  on an appropriate infrared cutoff  $k$ . These equations should reproduce the logarithmic four-dimensional running for  $k \gg T$  and exhibit the three-dimensional behaviour for  $k \ll T$ .

In this paper we perform this program for a pure scalar theory (the  $N$ -component  $\phi^4$  theory) as a first step towards the treatment of the standard model. We propose in the next section the average action [10,11] as an appropriate implementation of an infrared cutoff  $k$ . The average action  $\Gamma_k$  is the effective action for averages of fields over volumes  $k^{-d}$  (in  $d$  dimensions). It obtains after integrating out the modes with momenta larger than  $k$ . For  $k > 0$  no infrared divergence appears in the calculation of  $\Gamma_k$  since  $k$  acts as an infrared regulator. We study the evolution of the temperature dependent average potential as function of  $k$  and take the limit  $k \rightarrow 0$ . The couplings effectively run as a function of  $k$  only as long as some relevant mass  $m$  is smaller than  $k$ . For  $k \ll m$  the running stops and the mass  $m$  replaces  $k$  as an effective infrared cutoff. For massive theories the limit  $k \rightarrow 0$  can then be taken easily. Furthermore, our procedure remains valid even for vanishing mass. The three-dimensional fixed point structure in the running of the couplings cures the infrared divergences. This allows us to explore directly the behaviour at the critical temperature  $T_{\text{cr}}$ . Here the running with  $k$  is characterized by the fixed point of the three-dimensional theory.

Our method correctly describes the transition from the four-dimensional to the three-dimensional behaviour for  $k \gg T$  and  $k \ll T$  respectively. In addition, it provides the initial values of the couplings for their three-dimensional running and therefore allows for a quantitative treatment of the phase transition. For a small quartic coupling our results agree with high temperature perturbation theory for the behaviour of the potential at  $T \gg T_{\text{cr}}$  and for the determination of  $T_{\text{cr}}$ . On the other hand we find that high temperature perturbation theory breaks down for  $T$  near  $T_{\text{cr}}$ . In the vicinity of  $T_{\text{cr}}$  the true potential reflects the three-dimensional critical exponents. The phase transition is clearly second order and no “cubic term”  $\sim T(\phi^\dagger\phi)^{3/2}$  appears for  $\phi \rightarrow 0$ .

Compared to the diagrammatic methods of high temperature perturbation theory our method effectively includes additional contributions. The “daisy” or “ring” diagrams in high temperature perturbation theory lead to a replacement of the mass terms in the propagators by appropriate temperature and field dependent physical masses. These diagrams are taken into account in our method by the use of  $k$ ,  $T$  and field dependent masses in the propagators which appear in the evolution equations. The standard “daisy” diagrams would be reproduced by taking  $k = 0$  in the one loop expression (2.2) at  $T \neq 0$  with  $U(\rho, T)$  replac-

ing  $V$  on the right hand side. The evolution of  $U_k(\rho, T)$  as function of  $k$  with running masses and couplings sums up even more complicated diagrams which go beyond “daisy” graphs. (This is very similar to the usual renormalization group improvement.) The most important new contributions, however, come from an effective inclusion of higher order corrections to the four point vertex as expressed by the running of  $\lambda$ . They are not accounted for in previous treatments. These corrections are responsible for the vanishing of the cubic term at the critical temperature. Our “renormalization group improved” treatment leads to a correct description of the second order phase transition characterized by the critical exponents of the three-dimensional theory.

In sect. 2 we summarize the formalism of the average potential at zero temperature, concentrating on the techniques for its evaluation around the minimum. In sect. 3 we extend this formalism in order to take into account the non-zero temperature effects. In sect. 4 we study the evolution equations for the the non-zero temperature average potential of the four-dimensional  $N$ -component  $\phi^4$  theory. In sect. 5 we solve numerically the evolution equations and we obtain the full detailed picture of the phase transition. This section contains our main results: nature of the transition, critical temperature, very high temperature theory, critical exponents. In sect. 6 we obtain approximate analytic results which provide a deeper understanding and a check of the results of sect. 5. Our conclusions are presented in sect. 7.

## 2. The average potential

We present here a brief summary of the formalism of the average potential, concentrating on the techniques for its evaluation around the minimum. For a detailed presentation and discussion we refer the reader to refs. [10–13].

The average action in  $d$  dimensions is the effective action for averages of fields over a volume  $\sim k^{-d}$ . It describes the physics for systems which have a characteristic length scale  $k^{-1}$  by averaging out the degrees of freedom with momenta larger than  $k$ . The average potential  $U_k$  is real and does not have to be convex (as opposed to the effective potential). It can be shown [10] that  $U_k$  approaches the effective potential  $U$  as  $k \rightarrow 0$ . We concentrate in this paper on the  $N$ -component  $\phi^4$  theory in four dimensions and non-zero temperature. We neglect the wave function renormalization effects since the relevant anomalous dimensions are small [11]. A more detailed investigation, which includes the effects of the wave function renormalization, is under way [14].

The average potential around the minimum in  $d$  dimensions reads in the one loop approximation:

$$U_k(\rho) = V(\rho) + U_k^{(1)}(\rho), \quad (2.1)$$

where  $V(\rho)$  is the classical potential and the one loop contribution is given by

[10,12]

$$U_k^{(1)}(\rho) = \frac{1}{2}(2\pi)^{-d} \int d^d q \{ \ln(P(q) + V'(\rho) + 2V''(\rho)\rho) + (N - 1) \ln(P(q) + V'(\rho)) \}, \quad (2.2)$$

with

$$V'(\rho) = \frac{\partial V}{\partial \rho}, \quad \rho = \frac{1}{2} \phi^a \phi_a. \quad (2.3)$$

This is the same formula as in the standard loop expansion for the effective potential [7,2] (to which we refer as “naive” perturbation theory in the following), except that the inverse propagator  $q^2$  is now replaced by  $P(q)$ , with ( $a$  and  $b$  are constants of order 1):

$$P(q) = \frac{q^2}{1 - f_k^2(q)}, \quad (2.4)$$

$$f_k(q) = \exp \left\{ -a \left( \frac{q^2}{k^2} \right)^b \right\}. \quad (2.5)$$

This form of  $P$  provides for an effective infrared cutoff for all the modes with  $q^2 \ll k^2$ . In contrast, the contributions from the modes with  $q^2 \gg k^2$  are not modified. Only these modes are effectively integrated out in the computation of  $U_k$ . We note that for  $k \rightarrow 0$  one recovers directly the standard one loop contribution to the effective potential. The constants  $a$  and  $b$  determine the details of the averaging procedure. Since  $a$  can be absorbed in a redefinition of  $k$  we choose to work with a particular family of parametrizations [11,13]

$$b = \frac{\exp(2a) - 1}{2a}. \quad (2.6)$$

We want to derive evolution equations for the change of  $U_k$  with the scale  $k$  and follow these equations to  $k \rightarrow 0$ . This allows for an appropriate treatment of the infrared problems and, therefore, leads to an improved calculation of the effective potential  $U$ . For this purpose we take the logarithmic derivative with respect to  $k$  and substitute  $U_k$  for  $V$  in the integral (2.2). This “renormalization group improvement” [11] provides a partial resummation of higher loop contributions and results in the evolution equation ( $t = \ln(k/\Lambda)$ ,  $x = q^2$ ):

$$\begin{aligned} \frac{\partial}{\partial t} U_k(\rho) &= \frac{1}{2}(2\pi)^{-d} \int d^d q \frac{\partial P}{\partial t} \left( \frac{1}{P + U'_k(\rho) + 2U''_k(\rho)\rho} + \frac{N-1}{P + U'_k(\rho)} \right) \\ &= v_d \int_0^\infty dx x^{d/2-1} \frac{\partial P}{\partial t} \left( \frac{1}{P + U'_k(\rho) + 2U''_k(\rho)\rho} + \frac{N-1}{P + U'_k(\rho)} \right), \end{aligned} \quad (2.7)$$

with

$$v_d^{-1} = 2^{d+1} \pi^{d/2} \Gamma\left(\frac{d}{2}\right). \quad (2.8)$$

Eq. (2.7) is the master equation for our investigation. It connects the physics at the short distance cutoff ( $k = \Lambda$ ) with the long distance physics ( $k \rightarrow 0$ ). Its solution gives the effective potential  $U \equiv U_0$  (and therefore the ground state of the theory) in terms of the classical potential  $V \equiv U_\Lambda$ . We are interested in solving (2.7) around the minimum of the average potential. (For the calculation of the non-convex part see ref. [13].) In order to do so we parametrize  $U_k$  in terms of the location of its minimum and its successive derivatives with respect to  $\rho$  at the minimum. This results in an infinite system of coupled differential equations, which we solve approximately by truncation, keeping here only the second derivative.

In the *spontaneously broken regime* the average potential  $U_k$  has its minimum at  $\rho_0(k) \neq 0$ , determined by

$$U'_k(\rho_0) = 0. \quad (2.9)$$

We are interested in the scale dependence of  $\rho_0(k)$ , which is obtained by taking the  $t$ -derivative of (2.9)

$$U''_k(\rho_0(k)) \frac{d\rho_0(k)}{dt} = -\frac{\partial U'_k}{\partial t}(\rho_0(k)). \quad (2.10)$$

Here the partial derivative  $\partial U'_k/\partial t$  should be taken at fixed  $\rho_0(k)$ . We also define

$$\bar{\lambda}(k) = U''_k(\rho_0(k)). \quad (2.11)$$

The evolution equations for the scale dependence of  $\rho_0(k)$  and  $\bar{\lambda}(k)$  are easily derived by differentiation of (2.7) with respect to  $\rho$ . They read [10,11]:

$$\frac{d\rho_0}{dt} = -v_d k^{d-2} \{3L_1^d(2\bar{\lambda}\rho_0) + (N-1)L_1^d(0)\}, \quad (2.12)$$

$$\frac{d\bar{\lambda}}{dt} = -v_d k^{d-4} \bar{\lambda}^2 \{9L_2^d(2\bar{\lambda}\rho_0) + (N-1)L_2^d(0)\}, \quad (2.13)$$

with the dimensionless integrals  $L_n^d(w)$  given by

$$\begin{aligned} L_n^d(w) &= -nk^{2n-d} \pi^{-d/2} \Gamma\left(\frac{d}{2}\right) \int d^d q \frac{\partial P}{\partial t} (P+w)^{-(n+1)} \\ &= -nk^{2n-d} \int_0^\infty dx x^{d/2-1} \frac{\partial P}{\partial t} (P+w)^{-(n+1)}. \end{aligned} \quad (2.14)$$

In the *symmetric regime* ( $\rho_0(k) = 0$ ) we define:

$$m^2(k) = U'_k(0), \quad (2.15)$$

$$\bar{\lambda}(k) = U''_k(0), \quad (2.16)$$

and obtain the following evolution equations [13]:

$$\frac{dm^2}{dt} = (N + 2)v_d k^{d-2} \bar{\lambda} L_1^d(m^2), \tag{2.17}$$

$$\frac{d\bar{\lambda}}{dt} = - (N + 8)v_d k^{d-4} \bar{\lambda}^2 L_2^d(m^2). \tag{2.18}$$

The systems of equations (2.12), (2.13) and (2.17), (2.18) can be solved for given “short distance values”  $\rho_0(k = A)$  and  $\bar{\lambda}(k = A)$ . We start at the cutoff  $A$  and follow the renormalization group flow towards the infrared ( $k \rightarrow 0$ ). In this way we obtain the ground state of the theory  $\rho_0 \equiv \rho_0(k = 0)$ , as well as the renormalized couplings, mass terms etc. It should be noted that, even when one starts in the broken regime at  $k = A$ , it is possible that the evolution, as given by the first set of differential equations, may drive  $\rho_0(k)$  to zero at some non-zero  $k_s$ . From that point on the theory is in the symmetric regime and one has to continue the evolution using the second set of equations, with boundary conditions  $m^2(k_s) = 0$  and  $\bar{\lambda}(k_s)$  given by its value obtained from the running in the broken regime.

### 3. The non-zero temperature formalism

The discussion in the previous section has been carried in the zero temperature limit. In order to extend it to the non-zero temperature case we only need to recall that, in euclidean formalism, non-zero temperature  $T$  results in periodic boundary conditions in the time direction (for bosonic fields), with periodicity  $1/T$  [15]. This leads to a discrete spectrum for the zero component of the momentum  $q_0$

$$q_0 \rightarrow 2\pi mT, \quad m = 0, \pm 1, \pm 2, \dots \tag{3.1}$$

As a consequence the integration over  $q_0$  is replaced by summation over the discrete spectrum

$$\int \frac{d^d q}{(2\pi)^d} \rightarrow T \sum_m \int \frac{d^{d-1} \mathbf{q}}{(2\pi)^{d-1}}. \tag{3.2}$$

With the above remarks in mind we can easily generalize our master equation (2.7) in order to take into account the temperature effects. For the temperature dependent average potential  $U_k(\rho, T)$  we obtain:

$$\begin{aligned} \frac{\partial}{\partial t} U_k(\rho, T) &= \frac{1}{2} (2\pi)^{-(d-1)} T \sum_n \int d^{d-1} \mathbf{q} \frac{\partial P}{\partial t} \quad \text{---} \\ &\times \left( \frac{1}{P + U'_k(\rho, T) + 2U''_k(\rho, T)\rho} + \frac{N-1}{P + U'_k(\rho, T)} \right), \end{aligned} \tag{3.3}$$

with the implicit replacement

$$q^2 \rightarrow \mathbf{q}^2 + 4\pi^2 m^2 T^2 \tag{3.4}$$

in  $P$ . Again, the usual temperature dependent effective potential [2] obtains from  $U_k(\rho, T)$  in the limit  $k \rightarrow 0$ . As before, we can parametrize  $U_k(\rho, T)$  in terms of its minimum and its derivatives at the minimum. The evolution equations are given by (2.12), (2.13) and (2.17), (2.18), with the obvious generalizations

$$\begin{aligned} \rho_0(k) &\rightarrow \rho_0(k, T), \\ \bar{\lambda}(k) &\rightarrow \bar{\lambda}(k, T), \\ m^2(k) &\rightarrow m^2(k, T). \end{aligned} \tag{3.5}$$

The momentum integrals for non-vanishing temperature read:

$$L_n^d(w, T) = -nk^{2n-d} 2\pi^{-d/2+1} \Gamma\left(\frac{d}{2}\right) T \sum_m \int d^{d-1} \mathbf{q} \frac{\partial P}{\partial t} (P + w)^{-(n+1)}, \tag{3.6}$$

where the implicit replacement (3.4) is again assumed in  $P$ . These are crucial for the solution of the evolution equations and we next discuss them in detail.

The zero temperature integrals  $L_n^d(w)$ , given by (2.14), have been evaluated in references [11, 13] \*. For completeness we summarize the main results.  $L_n^d(w)$  has a pole at

$$w = -\bar{k}^2 \equiv -\frac{k^2}{1 - \exp(-2a)}, \tag{3.7}$$

for the family of parametrizations (2.6). The leading pole behaviour is  $\sim (w + \bar{k}^2)^{-(n+1/2)}$ . For  $w > -\bar{k}^2$ ,  $L_n^d$  is a monotonically decreasing function of  $w$ . Its value at  $w = 0$  can be calculated in closed form. Following [11] we define:

$$L_n^d(0) = -2l_n^d \tag{3.8}$$

and give the expressions for  $l_1^d, l_2^d$ , which will be useful in the following:

$$\begin{aligned} l_1^d &= (2a)^{-(d-2)/2b} \Gamma\left(1 + \frac{d-2}{2b}\right), \\ l_2^d &= (2a)^{-(d-4)/2b} \left(2 - 2^{-(d-4)/2b}\right) \Gamma\left(1 + \frac{d-4}{2b}\right). \end{aligned} \tag{3.9}$$

In this work we concentrate on  $w \geq 0$ . It is convenient to define the functions

$$S_n^d\left(\frac{w}{k^2}\right) = -\frac{L_n^d(w)}{2l_n^d}. \tag{3.10}$$

\* Since in this work we neglect wave function renormalization our expressions correspond to those of ref. [11] with the simplification  $Z = 1$ .

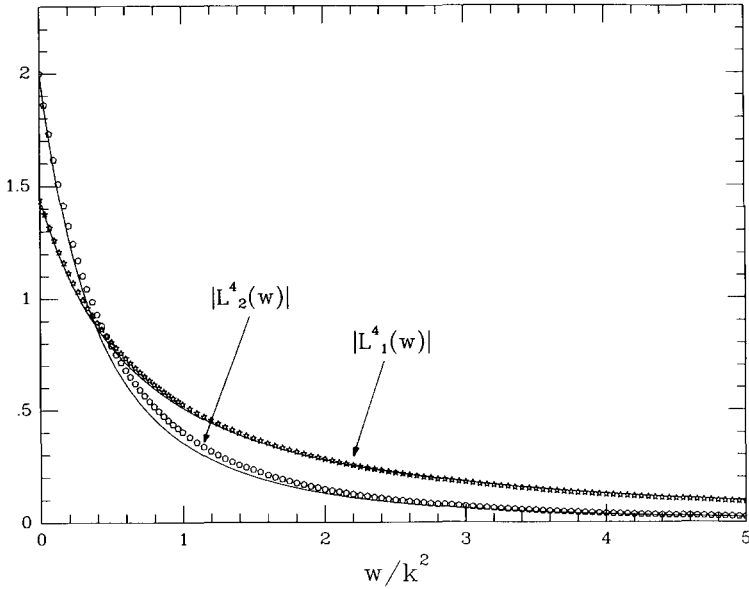


Fig. 1. The integrals  $L_1^4(w), L_2^4(w)$  for an average parameter  $b = 3$ . The points indicate the results of the numerical integration, while the continuous curves correspond to the approximate expression (3.11).

Their behaviour for moderate values of  $w/k^2$  is determined by the pole of  $L_n^d(w)$ . The approximation

$$s_n^d \left( \frac{w}{k^2} \right) \simeq \left( 1 + \frac{w}{k^2} \right)^{n+1/2} \tag{3.11}$$

agrees well with a numerical evaluation of the integrals. In fig. 1 we plot  $L_1^4, L_2^4$  as a function of  $w/k^2$ , for an average parameter  $b = 3$ . The results of the numerical integration are indicated by points, while the continuous lines correspond to the approximation of eq. (3.11). Similar results for  $L_1^3, L_2^3$  are presented in fig. 2. Since  $L_n^d(w)$  does not have a simple analytic form we have performed numerical fits of the points shown in figs. 1 and 2 which we use for the numerical solution of the differential evolution equations.

We turn now to the evaluation of the non-zero temperature integrals  $L_n^d(w, T)$ , which are given by the expression (3.6). Their basic properties can be established analytically. For  $T \ll k$  the summation over discrete values of  $m$  in expression (3.6) is equal to the integration over a continuous range of  $q_0$  up to exponentially small corrections. Therefore

$$L_n^d(w, T) = L_n^d(w) \quad \text{for } T \ll k. \tag{3.12}$$

In the opposite limit  $T \gg k$  the summation over  $m$  is dominated by the

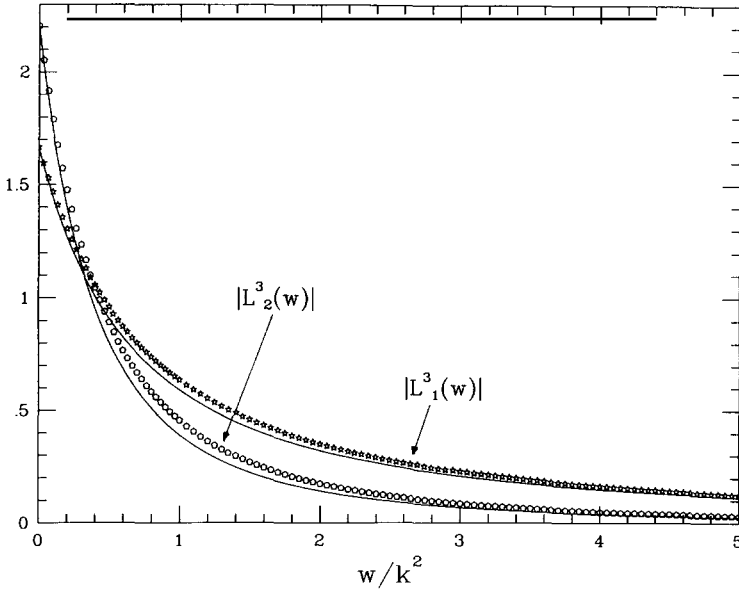


Fig. 2. The integrals  $L_1^3(w), L_2^3(w)$  for an average parameter  $b = 3$ . The points indicate the results of the numerical integration, while the continuous curves correspond to the approximate expression (3.11).

$m = 0$  contribution. Terms with non-zero values of  $m$  are suppressed by  $\sim \exp(- (mT/k)^{2b})$ . The leading contribution gives the simple expression

$$L_n^d(w, T) = \frac{v_{d-1}}{v_d} \frac{T}{k} L_n^{d-1}(w) \quad \text{for } T \gg k, \quad (3.13)$$

with  $v_d$  defined in (2.8). The two regions of  $T/k$  in which  $L_n^d(w, T)$  is given by eqs. (3.12), (3.13) are connected by a small interval in which the exponential corrections result in complicated dependence on  $w$  and  $T$ .

The above conclusions are verified by a numerical calculation of  $L_1^4(w, T)$  and  $L_2^4(w, T)$ . In fig. 3 we plot  $L_1^4(w, T)/L_1^4(w)$  as a function of  $T/k$ , for various values of  $w/k^2$  and for  $b = 3$ . The behaviour of  $L_2^4(w, T)$  is presented in fig. 4. We distinguish three regions:

(a)  $T/k \leq \theta_1$ : This is the *low temperature region* where  $L_{1,2}^4(w, T)$  are very well approximated by their zero temperature value. We take  $\theta_1 = 0.05$  and use  $L_n^4(w, 0)$  in the evolution equations for  $k \geq T/\theta_1$ .

(b)  $\theta_1 < T/k < \theta_2$ : In the *threshold region* we perform a numerical fit of the curve corresponding to  $w = 0$  which we use for all values of  $w$ . This is a very good approximation since the relevant  $w/k^2$  turns out to be small in this region (see next sections). We determine  $\theta_2$  by the value of  $T/k$  at which the

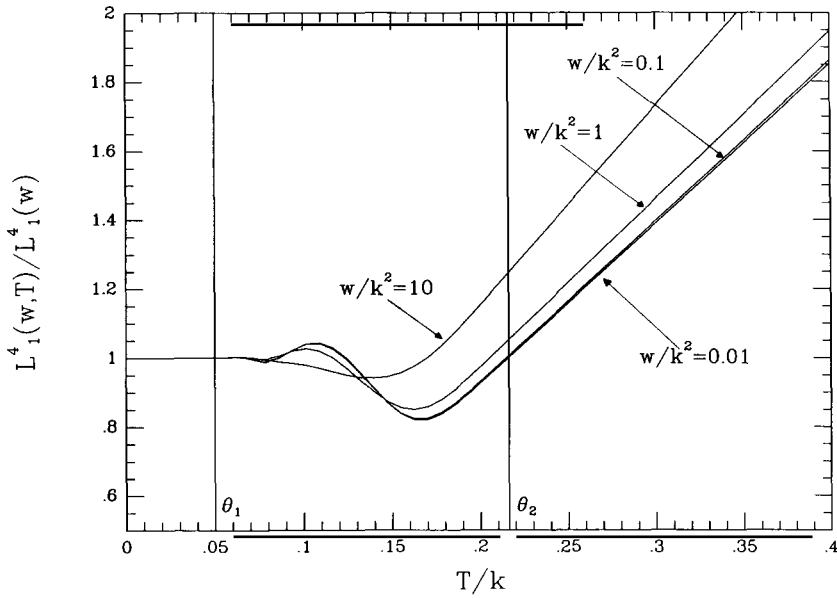


Fig. 3.  $L_1^4(w, T)/L_1^4(w)$  as a function of  $T/k$ , for various values of  $w/k^2$  ( $b = 3$ ).

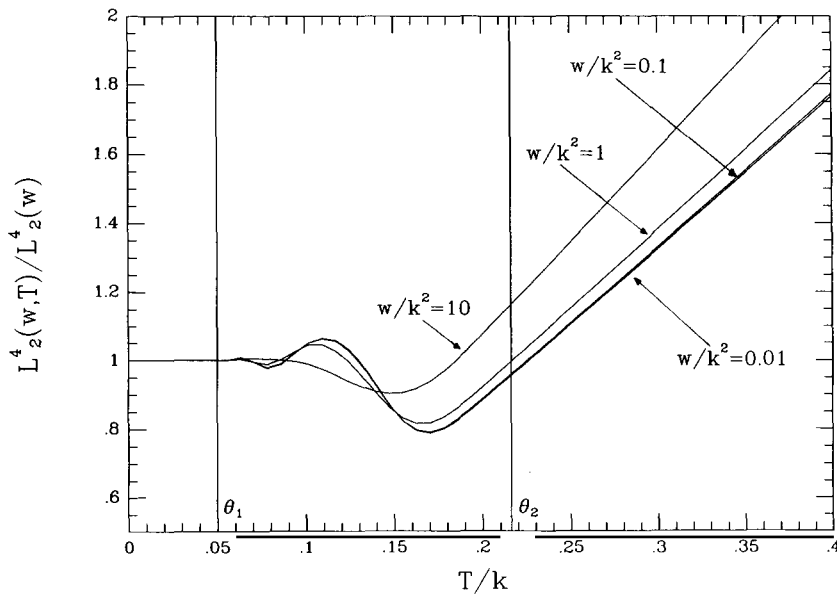


Fig. 4.  $L_2^4(w, T)/L_2^4(w)$  as a function of  $T/k$ , for various values of  $w/k^2$  ( $b = 3$ ).

high temperature expression for  $L_1^4(0, T)$  becomes equal to  $L_1^4(0)$ . This gives (for  $b = 3$ ):

$$\theta_2 = \frac{l_1^4}{4l_1^3} \simeq 0.216. \quad (3.14)$$

(c)  $T/k \geq \theta_2$ : For the *high temperature region* we use for the numerical solution of the evolution equations

$$L_{1,2}^4(w, T) = 4 \frac{T}{k} L_{1,2}^3(w). \quad (3.15)$$

The three dimensional character of the effective theory for modes with  $q^2 \ll T^2$  manifests itself in the appearance of the three dimensional momentum integrals. It acquires here a precise quantitative meaning.

#### 4. Running in four and three dimensions

We can now apply the formalism developed in the previous sections to the study of the evolution equations for the four-dimensional  $\phi^4$  theory at non-vanishing temperature. We consider the models with spontaneous symmetry breaking at zero temperature, and investigate the restoration of symmetry as the temperature is raised. We specify the action together with some high momentum cutoff  $\Lambda \gg T$  such that the theory is properly regulated. We then solve the evolution equation (3.3) for  $k \rightarrow 0$  for different values of the temperature. This provides all relevant features of the temperature dependent effective potential.

In order to solve the evolution equations we have to specify appropriate boundary conditions. These can be determined by the “short distance values”  $\rho_0(k = \Lambda)$  and  $\lambda(k = \Lambda)$  \* which correspond to the minimum and the quartic coupling of the classical potential. We then have to compute the evolution of the quantities (3.5), starting at  $k = \Lambda$  and following the renormalization flow towards  $k = 0$ . This procedure has to be followed for  $T = 0$  and then to be repeated for  $T \neq 0$  in order to relate the zero and non-zero temperature effective potential of the same theory (as specified by the parameters at the cutoff). Since the running of the parameters is the same in the zero and non-zero temperature case for  $k \geq T/\theta_1 = 20T$  we actually do not need to compute the evolution in this range of  $k$ . Our strategy is equivalent to the following procedure: We start with the zero temperature theory at  $k = 0$  taking the renormalized parameters (see below) as input. We subsequently integrate the zero temperature evolution equations “up” to  $k = T/\theta_1$ . We can now use the values of the running parameters at  $k = T/\theta_1$  as initial conditions for the non-zero temperature evolution equations and integrate them “down” to  $k = 0$ . In this way we obtain the

\* When neglecting wave function renormalization, the definitions (2.11), (2.16) coincide, in four dimensions, with the renormalized quartic coupling. For this reason we omit the bar on  $\lambda$  from here on.

renormalized parameters at non-zero temperature in terms of the renormalized parameters at zero temperature. More specifically, we integrate first the evolution equations from  $k = T/\theta_1$  to  $k = T/\theta_2$  using the numerical fit of the  $L$  integrals in this threshold region. This gives the initial conditions for the running between  $k = T/\theta_2$  and  $k = 0$  where we use the high temperature approximation (3.15) for the  $L$  integrals. In this range of  $k$  the running is determined by the evolution equations of the three-dimensional theory. By neglecting the difference between  $L_n^A(w)$  and  $L_n^A(w, T)$  for  $T/\theta_2 < k < T/\theta_1$  our procedure simplifies even further. It may be summarized as “run up in four dimensions, run down in three dimensions”, with a matching of the  $k$ -dependent couplings at the scale  $T/\theta_2$ . In practice we shall take the “threshold correction” from the different running for  $T/\theta_2 < k < T/\theta_1$  into account. We find that this gives only a small modification. In the case that  $\rho_0(k, T)$  becomes zero at some non-zero  $k_s$  we continue with the equations for the symmetric regime with boundary conditions  $m^2(k_s, T) = 0$  and  $\lambda(k_s, T)$  given by its value at the end of the running in the spontaneously broken regime.

One last remark concerns the definition of the renormalized couplings for the zero temperature theory. Due to the presence of Goldstone modes for  $N > 1$  the four-dimensional theory is infrared free ( $\lim_{k \rightarrow 0} \lambda(k) = 0$ ) in the spontaneously broken phase. This holds even for a finite momentum cutoff  $\Lambda$ . In contrast, the running of  $\lambda(k)$  is stopped by the scalar mass for  $N = 1$  or in the symmetric phase. Even though the logarithmic running  $\lambda(k) \rightarrow 0$  is very slow we cannot define the renormalized quartic coupling by the appropriate derivative of the effective potential for  $k \rightarrow 0$ . Instead, we could define the quartic coupling at non-zero external momentum. In our context, it is more convenient to use  $\lambda(k)$  at some non-vanishing scale  $k = k_0$ , which we choose equal to the mass of the radial scalar mode i.e.  $k_0^2 = 2\lambda(k_0)\rho_0(0)$ . This definition is clearly related to a definition by the four-point function with momenta  $p^2 \simeq k_0^2$ . For reasons of uniformity we preserve the same definition of the renormalized  $\lambda$  in the case  $N = 1$ . (For  $N = 1$  the residual running of  $\lambda(k)$  (from  $k_0$  to zero) is negligible for the range of parameters of interest.) We also use the following notation for the renormalized quantities:

$$\begin{aligned} \rho_0 &= \rho_0(0), \\ \lambda_R &= \lambda(k_0) = \lambda(\sqrt{2\lambda_R\rho_0}). \end{aligned} \tag{4.1}$$

Here  $\rho_0$  corresponds to the minimum of the average potential in the limit  $k \rightarrow 0$ , such that  $\rho_0^{1/2}$  is the vacuum expectation value of the zero temperature theory. We also remind that “triviality” of the  $\phi^4$  theory implies the necessity of some physical ultraviolet cutoff if  $\lambda(k_0) > 0$ . Following the four-dimensional evolution equations implies that  $\lambda(k)$  diverges for some critical scale  $k_{cr}$ . Our investigation makes sense as long as the temperature is small compared to  $k_{cr}$  so that

we can choose  $A \leq k_{\text{cr}}$ .

Having set up our strategy, we next cast the evolution equations in a form which is suitable for the numerical or analytical solution.

(a) For the four-dimensional zero temperature running (or low temperature running  $T/k \leq \theta_1$ ) the evolution equations are given by (2.12), (2.13). It is convenient to define the dimensionless quantity

$$\kappa(k) = \frac{\rho_0(k)}{k^2}. \quad (4.2)$$

Recalling the definitions (3.8) and (3.10) one can eliminate any explicit  $k$  dependence on the right-hand-side

$$\frac{d\kappa}{dt} = -2\kappa + \frac{1}{16\pi^2} l_1^4 \{N - 1 + 3s_1^4(2\lambda\kappa)\}, \quad (4.3)$$

$$\frac{d\lambda}{dt} = \frac{1}{16\pi^2} l_2^4 \lambda^2 \{N - 1 + 9s_2^4(2\lambda\kappa)\}. \quad (4.4)$$

(b) In the threshold region  $\theta_1 < T/k < \theta_2$  we define

$$r_n^4(T/k) = \frac{L_n^4(0, T)}{L_n^4(0)},$$

$$\kappa(k, T) = \frac{\rho_0(k, T)}{k^2}. \quad (4.5)$$

For small enough  $\lambda_R$  one finds in this region (see next sections)  $\kappa(k, T)$   $\lambda(k, T) \ll 1$ . It is, therefore, a good approximation to assume that  $r_n^4(T/k)$  gives the non-zero temperature corrections to  $L_n^4(w)$  for all relevant values of  $w$ . With this assumption we obtain for the intermediate range the following equations:

$$\frac{d\kappa}{dt} = -2\kappa + \frac{1}{16\pi^2} l_1^4 r_1^4 \{N - 1 + 3s_1^4(2\lambda\kappa)\}, \quad (4.6)$$

$$\frac{d\lambda}{dt} = \frac{1}{16\pi^2} l_2^4 r_2^4 \lambda^2 \{N - 1 + 9s_2^4(2\lambda\kappa)\}. \quad (4.7)$$

For the numerical solution of the above equations we use a numerical fit of the functions  $r_1^4(T/k)$ ,  $r_2^4(T/k)$ .

(c) In the high temperature region  $T/k \geq \theta_2$ , use of the expression (3.15) results in the following equations:

$$\frac{d\rho'_0}{dt} = -v_3 k \{3L_1^3(2\lambda'\rho'_0) + (N - 1)L_1^3(0)\}, \quad (4.8)$$

$$\frac{d\lambda'}{dt} = -v_3 k^{-1} (\lambda')^2 \{9L_2^3(2\lambda'\rho'_0) + (N - 1)L_2^3(0)\}, \quad (4.9)$$

with

$$\begin{aligned} \rho'_0(k, T) &= \frac{\rho_0(k, T)}{T}, \\ \lambda'(k, T) &= \lambda(k, T)T. \end{aligned} \tag{4.10}$$

Comparison with (2.12), (2.13) shows that the above equations are exactly the ones of the three-dimensional theory for the effective three-dimensional couplings  $\rho'_0(k, T), \lambda'(k, T)$ . We recover the fact that the behaviour of the high temperature four-dimensional theory is determined by the zero temperature three-dimensional theory. Moreover, we have developed a formalism which connects the four-dimensional regime with the effective three-dimensional one in a quantitative way. This is crucial since the precise initial values of the three-dimensional running are needed for the determination of the critical temperature etc.

It is convenient again to define the dimensionless quantities

$$\begin{aligned} \tilde{\kappa}(k, T) &= \frac{\rho'(k, T)}{k} = \frac{\rho_0(k, T)}{kT}, \\ \tilde{\lambda}(k, T) &= \frac{\lambda'(k, T)}{k} = \lambda(k, T) \frac{T}{k}. \end{aligned} \tag{4.11}$$

In terms of these quantities the evolution equations read:

$$\frac{d\tilde{\kappa}}{dt} = -\tilde{\kappa} + \frac{1}{4\pi^2} l_1^3 \{N - 1 + 3s_1^3 (2\tilde{\lambda}\tilde{\kappa})\}, \tag{4.12}$$

$$\frac{d\tilde{\lambda}}{dt} = -\tilde{\lambda} + \frac{1}{4\pi^2} l_2^3 \tilde{\lambda}^2 \{N - 1 + 9s_2^3 (2\tilde{\lambda}\tilde{\kappa})\}. \tag{4.13}$$

The main qualitative difference of the last equations compared to equations (4.3), (4.4) arises from the term  $-\tilde{\lambda}$  on the right-hand side of (4.13), which is due to the dimensions of  $\lambda'$ . In consequence, the dimensionless quartic coupling  $\tilde{\lambda}$  is not infrared free. Its behaviour with  $k \rightarrow 0$  is characterized by an approximate fixed point for the region where  $\tilde{\kappa}$  varies only slowly. Taken together, the pair of differential equations for  $(\tilde{\lambda}, \tilde{\kappa})$  has an exact fixed point  $(\tilde{\kappa}_{fp}, \tilde{\lambda}_{fp})$  corresponding to the phase transition [11]. This can be demonstrated explicitly by the numerical solution of (4.12), (4.13). The phase diagrams for  $N = 1$  and  $N = 4$  are plotted in figs. 5 and 6, respectively. There is a critical line separating the spontaneously broken from the symmetric phase. We also have indicated the flow of the couplings for decreasing  $k$ . In table 1 we list the fixed points of (4.12), (4.13) for various values of  $N$  and  $b = 3$ .

We also need the evolution equations in the symmetric regime at non-zero temperature. Their derivation is straightforward by means of (2.17), (2.18), (3.15). By defining the dimensionless quantity

$$\tilde{m}^2(k, T) = \frac{m^2(k, T)}{k^2}, \tag{4.14}$$

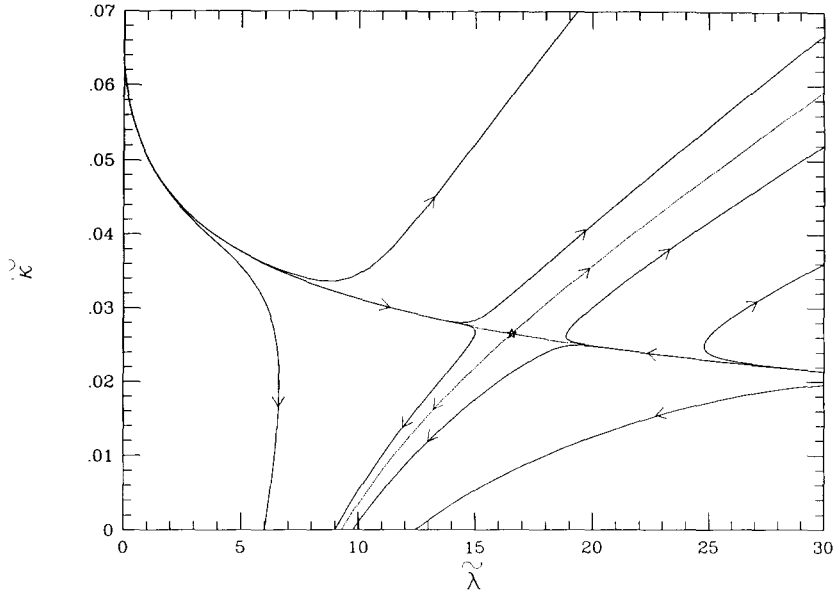


Fig. 5. The phase diagram of the three-dimensional theory for  $N = 1$  ( $b = 3$ ).

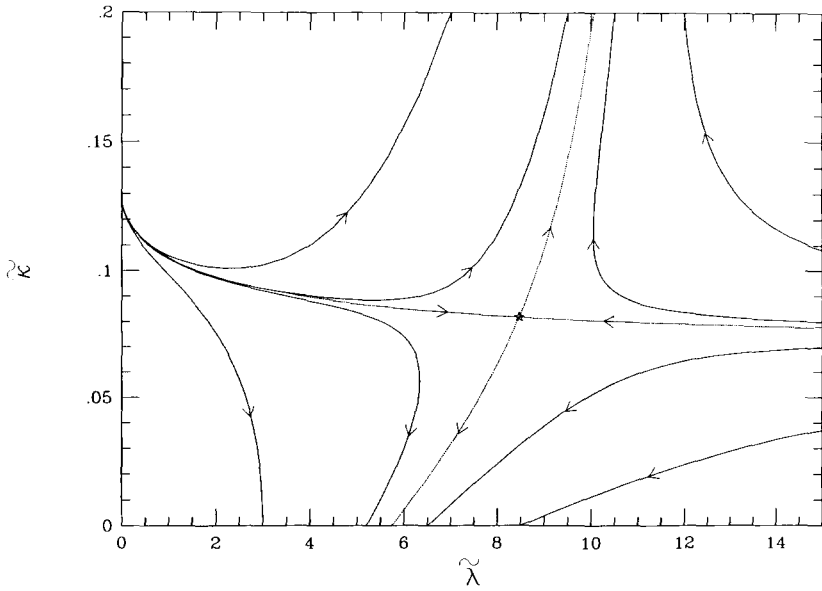


Fig. 6. The phase diagram of the three-dimensional theory for  $N = 4$  ( $b = 3$ ).

TABLE 1

Fixed points of the zero temperature three-dimensional evolution equations for various  $N$  ( $b = 3$ )

$N$	1	3	4	10
$\tilde{\kappa}_{\text{fp}}$	0.027	0.062	0.082	0.208
$\tilde{\lambda}_{\text{fp}}$	16.56	10.89	8.48	3.53

we obtain:

$$\frac{d\tilde{m}^2}{dt} = -2\tilde{m}^2 - \frac{1}{4\pi^2} l_1^3 \tilde{\lambda} (N + 2) s_1^3(\tilde{m}^2), \tag{4.15}$$

$$\frac{d\tilde{\lambda}}{dt} = -\tilde{\lambda} + \frac{1}{4\pi^2} l_2^3 \tilde{\lambda}^2 (N + 8) s_2^3(\tilde{m}^2). \tag{4.16}$$

Before presenting the results of the numerical solution of the evolution equations (4.3), (4.4), (4.6), (4.7), (4.12), (4.13), (4.15), (4.16), we consider a simplified approach which will be useful in sect. 6 where approximate analytic results will be derived. As we have explained in the beginning of this section, the threshold region interpolates between the regions of four-dimensional and three-dimensional running. A more simplified approach would neglect this region and consider only the “running up in four dimensions” and “running down in three dimensions”, with a matching of  $\kappa, \lambda$  at the scale  $k_T = T/\theta_2$ . For sufficiently small  $\lambda_R$  we can take into account the effect of the threshold region by considering a “threshold correction” to the matching of  $\kappa, \lambda$  at  $k_T$ . More specifically, for the interval  $T/\theta_2 < k < T/\theta_1$ , we calculate the difference between the zero temperature evolution of  $\kappa, \lambda$  as given by (4.3), (4.4), and the evolution given by (4.6), (4.7). For small  $\lambda_R$  we can neglect the difference in the running of  $\lambda$  and use the approximation  $s_1^4 = 1$ . As a result the difference in running for  $\kappa$  can be cast in the form

$$\delta\kappa = \kappa(T/\theta_2, T) - \kappa(T/\theta_2, 0) = \frac{N + 2}{2} \mathcal{A}. \tag{4.17}$$

The parameter  $\mathcal{A}$  is independent of  $T$  and  $\lambda$  in leading order and can be calculated numerically. For  $b = 3$  we find:

$$\mathcal{A} = 6.59 \times 10^{-4}. \tag{4.18}$$

We can therefore use the simplified picture in order to derive approximate results. It involves “running up in four dimensions” from  $k = 0$  to  $k_T = T/\theta_2$  and “running down in three dimensions” from  $k_T = T/\theta_2$  to  $k = 0$ . The values of  $\kappa, \lambda$  are matched at  $k_T$ , with a “threshold correction” for  $\kappa$  given by (4.17), (4.18).

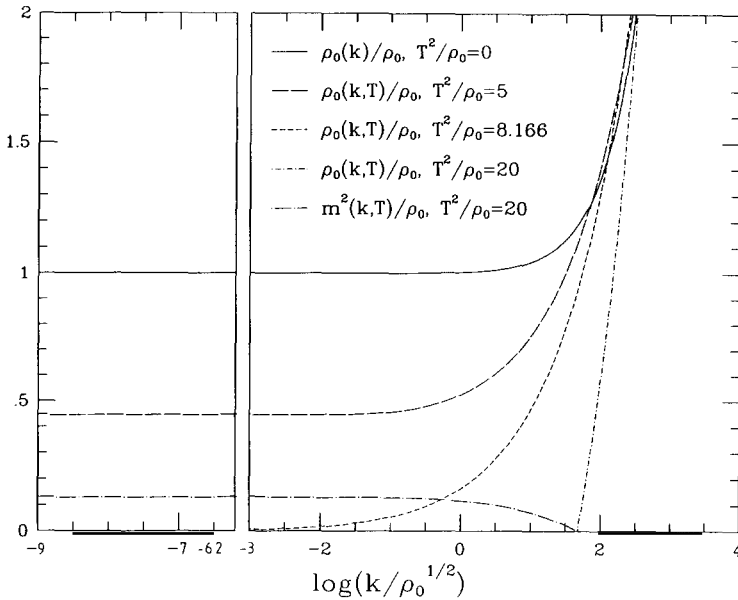


Fig. 7. The evolution of  $\rho_0$  at various temperatures. For  $T > T_{cr}$  the evolution of the mass term in the symmetric regime is also displayed.  $N = 1, \lambda_R = 0.1, b = 3$ .

### 5. The phase transition

The results of the numerical integration of the evolution equations (4.3), (4.4), (4.6), (4.7), (4.12), (4.13), (4.15), (4.16) are presented in figs. 7,8 and 9,10 for  $N = 1$  and  $N = 4$ , respectively ( $\lambda_R = 0.1$ ). The solid line in figs. 7, 9 displays the “quadratic renormalization” [10,11] of the minimum of the zero temperature average potential. At non-zero temperature (dashed lines) we notice the deviation from the zero temperature behaviour. It starts at  $k = T/\theta_1$  and we first observe the complicated running in the threshold region  $T/\theta_2 \leq k \leq T/\theta_1$ . For low temperatures, in the limit  $k \rightarrow 0$ ,  $\rho_0(k, T)$  reaches an asymptotic value  $\rho_0(0, T) < \rho_0$ . This value corresponds to the vacuum expectation value of the non-zero temperature theory and we denote it by

$$\rho_0(T) = \rho_0(0, T). \tag{5.1}$$

At a specific temperature  $T_{cr}$ ,  $\rho_0(T)$  becomes zero and this signals the restoration of symmetry for  $T \geq T_{cr}$ . The running of  $\lambda(k), \lambda(k, T)$  is shown in figs. 8 and 10 for  $N = 1$  and  $N = 4$ . We observe the logarithmic running of  $\lambda(k)$  (solid line) which is stopped by the mass term in the  $N = 1$  case. For non-zero temperatures  $\lambda(k, T)$  deviates from the zero temperature running. For  $N = 1$  it reaches a non-zero value in the limit  $k \rightarrow 0$ , while in the  $N = 4$  case it approaches zero  $\sim k$ .

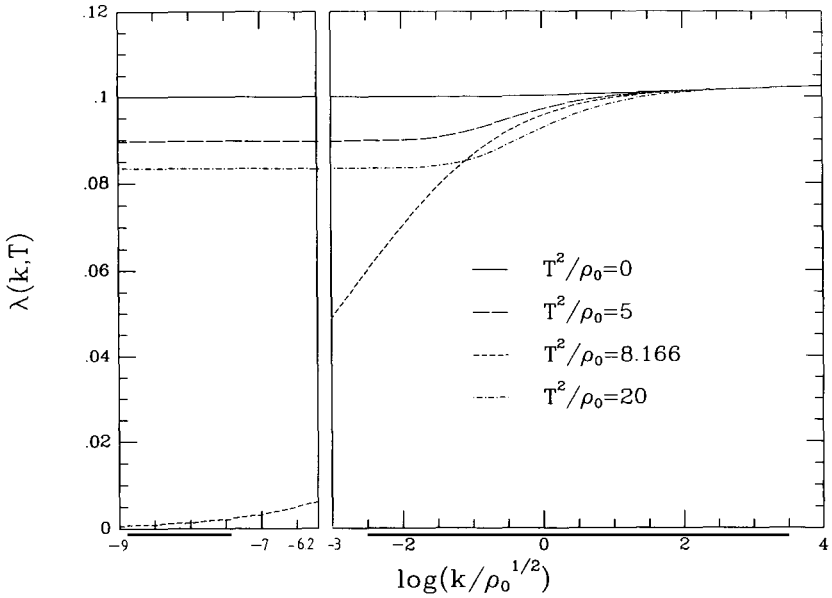


Fig. 8. The evolution of  $\lambda$  at various temperatures.  $N = 1, \lambda_R = 0.1, b = 3$ .

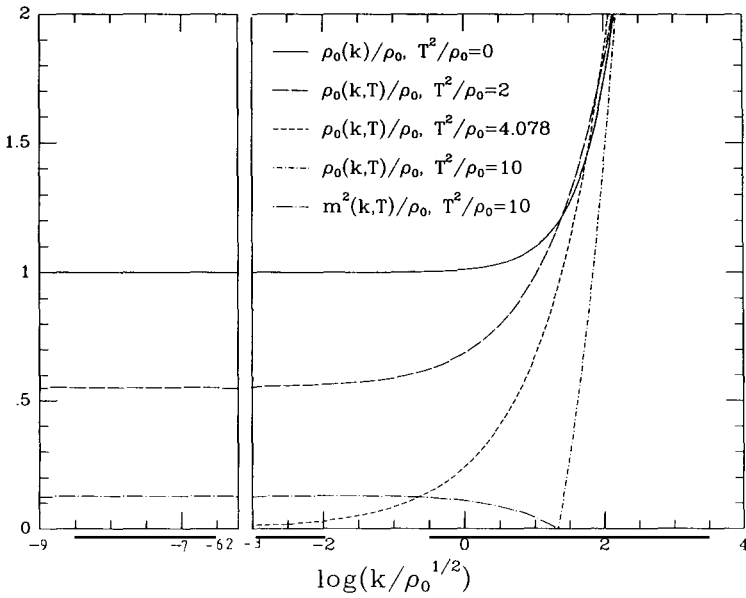


Fig. 9. The evolution of  $\rho_0$  at various temperatures. For  $T > T_{cr}$  the evolution of the mass term in the symmetric regime is also displayed.  $N = 4, \lambda_R = 0.1, b = 3$ .

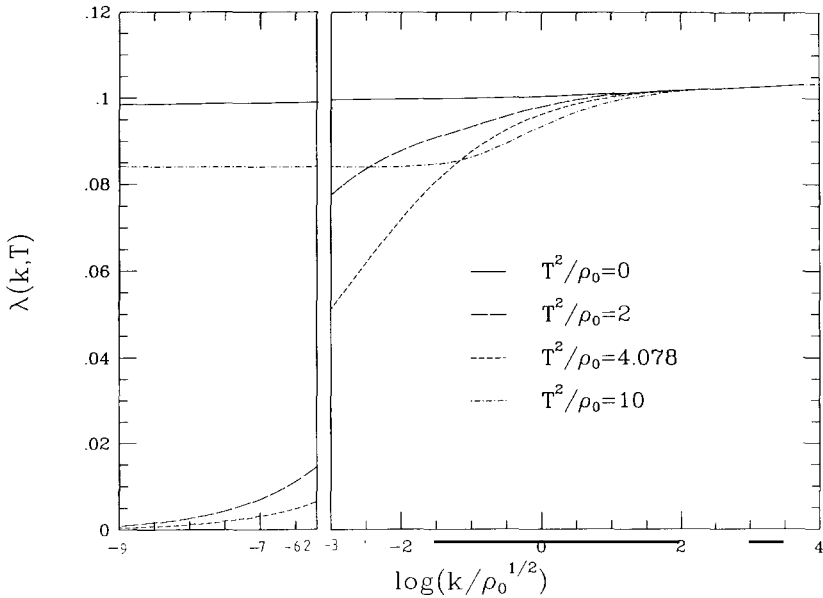


Fig. 10. The evolution of  $\lambda$  at various temperatures.  $N = 4, \lambda_R = 0.1, b = 3$ .

The latter effect is due to the fluctuations of the massless Goldstone bosons. In both cases  $\lambda(k, T)$  runs to zero for  $T \rightarrow T_{\text{cr}}$ . We see that the problem of the definition of the renormalized coupling reappears for the non-zero temperature theory in the spontaneously broken phase. In analogy to (4.1) we define  $\lambda_R(T)$  at a non-zero scale

$$\lambda_R(T) = \lambda(\sqrt{2\lambda_R(T)\rho_0(T)}, T) \quad (5.2)$$

in the spontaneously broken phase for all values of  $N$ . For  $T > T_{\text{cr}}$  the running in the spontaneously broken regime ends at a non-zero  $k_s$ , at which  $\rho_0(k_s, T)$  equals zero. From this point on we continue the evolution in the symmetric regime. The running of  $m^2(k, T)$  is depicted in figs. 7, 9 while the evolution of  $\lambda(k, T)$  proceeds continuously in the new regime as shown in figs. 8, 10. In the symmetric phase the theory is not infrared free and we define:

$$\begin{aligned} m_R^2(T) &= m^2(0, T), \\ \lambda_R(T) &= \lambda(0, T). \end{aligned} \quad (5.3)$$

The procedure of “running up in four dimensions” and “running down in three dimensions” provides the connection between the renormalized quantities at zero and non-zero temperature. We define the zero temperature theory in terms of the location of the minimum  $\rho_0$  and the renormalized quartic coupling  $\lambda_R$ .

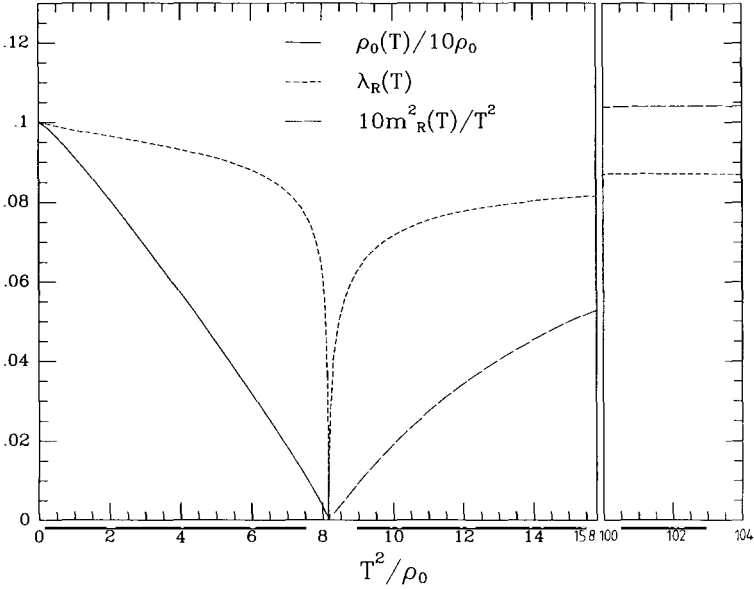


Fig. 11.  $\rho_0(T), \lambda_R(T), m_R^2(T)$  for a wide range of temperatures.  $N = 1, \lambda_R = 0.1, b = 3$ .

Through the solution of the evolution equations we obtain  $\rho_0(T)$  and  $\lambda_R(T)$  for non-zero temperatures  $T < T_{cr}$ . For  $T \geq T_{cr}$  the symmetry is restored ( $\rho_0(T) = 0$ ) and the non-zero temperature theory is described in terms of  $m_R^2(T)$  and  $\lambda_R(T)$ . In figs. 11, 12 we plot  $\rho_0(T)/\rho_0, \lambda_R(T)$  and  $m_R^2(T)/T^2$  as a function of temperature, for  $N = 1$  and  $N = 4$  respectively and  $\lambda_R = 0.1$ . As the temperature increases towards  $T_{cr}$  we observe a continuous transition from the spontaneously broken to the symmetric phase. This clearly indicates a *second order phase transition*. The renormalized quartic coupling  $\lambda_R(T)$  remains close to its zero temperature value  $\lambda_R$  for a large range of temperatures and drops quickly to zero at  $T = T_{cr}$ . Recalling our parametrization of the average potential in terms of its successive  $\rho$  derivatives at the minimum, we conclude that, at  $T_{cr}$ , the first non-zero term in the expression for the effective potential is the  $\phi^6$  term (which we have neglected in our truncated solution). For  $T \gg T_{cr}$  the coupling  $\lambda_R(T)$  quickly grows to approximately its zero temperature value  $\lambda_R$ , while  $m_R^2(T)$  asymptotically becomes proportional to  $T^2$  as  $T \rightarrow \infty$ . In the symmetric phase the quartic coupling is finite for all temperatures and vanishes for  $T \rightarrow T_{cr}$ . No “cubic term”  $\sim T\phi^3$  appears. (Its presence would have resulted in the divergence of  $\lambda_R(T)$  for  $T \rightarrow T_{cr}$ .)

Having presented the general features of the non-zero temperature theory, we now turn to a more detailed quantitative discussion. The value of the critical

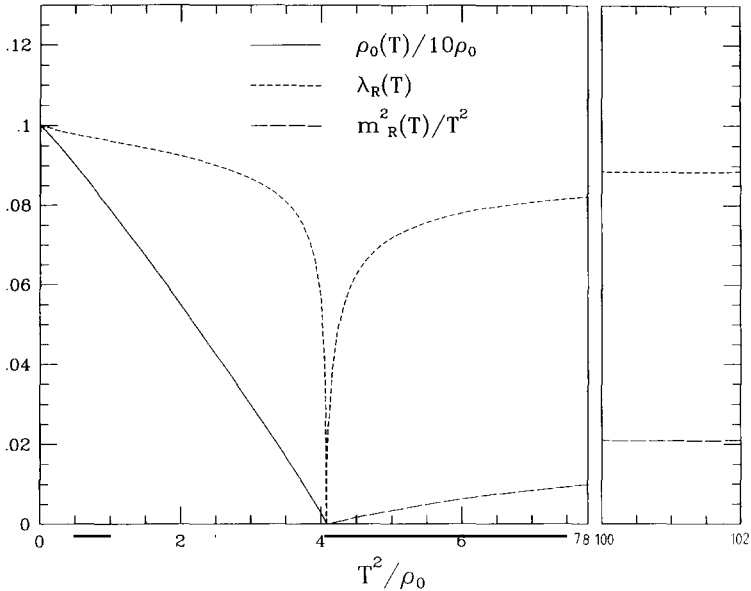


Fig. 12.  $\rho_0(T), \lambda_R(T), m_R^2(T)$  for a wide range of temperatures.  $N = 4, \lambda_R = 0.1, b = 3$ .

TABLE 2

$T_{cr}^2(N + 2)/\rho_0$  for various values of  $\lambda_R$  and  $N$ .  $b = 3$ . “Naive” perturbation theory gives  $T_{cr}^2(N + 2)/\rho_0 = 24$

$N$	$\lambda_R = 0.01$	$\lambda_R = 0.1$	$\lambda_R = 1$
1	24.05	24.50	26.82
3	24.03	24.48	26.70
4	24.03	24.48	26.61
10	24.02	24.42	26.10

temperature  $T_{cr}$  in terms of the zero temperature quantities has been calculated in the context of “naive” perturbation theory [1–3]. It was found that  $T_{cr}$  is given by  $T_{cr}^2 = [24/(N + 2)]\rho_0$ , independent of  $\lambda_R$  in lowest order. In table 2 we list the quantity  $T_{cr}^2/(N + 2)\rho_0$  for various values of  $N$  and  $\lambda_R$ . We observe excellent agreement with “naive” perturbation theory for  $\lambda_R \rightarrow 0$ , and significant deviations for larger  $\lambda_R$ . This is not surprising if one recalls that  $T_{cr}$  is calculated as the temperature at which the mass term  $m_R^2(T)$  becomes zero. For the calculation of  $m_R^2(T)$  Dolan and Jackiw [2] summed the dominant class of higher order “daisy” graphs in the large  $N$  limit and showed that they do not modify the one loop expression for  $T_{cr}$ . This procedure correctly reproduces the main effect of the evolution of  $\rho_0(k, T)$  in our scheme. The higher loop corrections to  $\lambda_R(T)$

TABLE 3

$[m_R^2(T)/\lambda_R(T)(N + 2)T^2]^{-1}$  for  $T^2/\rho_0 = 10^6$  and various values of  $\lambda_R$  and  $N$ .  $b = 3$ . “Naive” perturbation theory gives  $[m_R^2(T)/\lambda_R(T)(N + 2)T^2]^{-1} = 24$  for  $T^2/\rho_0 \rightarrow \infty$

$N$	$\lambda_R = 10^{-4}$	$\lambda_R = 0.01$	$\lambda_R = 0.1$
1	23.92	23.62	23.19
3	23.94	23.91	24.02
4	23.95	24.01	24.32
10	23.99	24.40	25.53

were not considered. In our scheme this is equivalent to neglecting the evolution of  $\lambda(k, T)$ . This effect is responsible for the deviations from the “naive” perturbative prediction for large  $\lambda_R$ . In particular, in our scheme, the critical temperature is obtained through the initial values of  $\tilde{\kappa}, \tilde{\lambda}$  (defined in (4.11)) at the scale  $k_T = T/\theta_2$ , which determine the nature of the effective three dimensional running in the high temperature region. (For a detailed discussion see sect. 6). Whether the theory will evolve to the spontaneously broken or the symmetric phase is determined by the location of the point  $(\tilde{\kappa}(k_T, T), \tilde{\lambda}(k_T, T))$  above or below the critical line (see figs. 5 and 6). In the limit  $\lambda_R \rightarrow 0$ ,  $\lambda(k_T, T)$  is simply equal to  $\lambda_R$ , since the running in the zero temperature and threshold regions is negligible. Also the value of  $\tilde{\kappa}(k_T, T)$  becomes independent of  $\lambda_R$  and is given by the ultraviolet fixed point of eq. (4.12) with  $s_1^3 = 1$ . In this limit the “naive” perturbative result should be reliable.

Another quantity which can be compared with the “naive” perturbative predictions is  $m_R^2(T)$  in the limit  $T \rightarrow \infty$ . In table 3 we list the results of our calculation for the expression  $[m_R^2(T)/\lambda_R(T)(N + 2)T^2]^{-1}$  for  $T^2/\rho_0 = 10^6$ . The “naive” perturbative result for this quantity is 24, independent of  $N$  and  $\lambda_R$ . We find again excellent agreement for  $\lambda_R \rightarrow 0$ , which can be traced to the absence of significant evolution for  $\lambda(k, T)$ . (More details on the analytic calculation of  $m_R^2(T)$  are given in sect. 6.)

The most important aspect of our calculation is related to the infrared behaviour of the theory for  $T \rightarrow T_{cr}$ . The temperature dependence of  $\rho_0(T)$ ,  $\lambda_R(T)$ ,  $m_R^2(T)$  near  $T_{cr}$  is presented in figs. 13 and 14 for  $N = 1$  and  $N = 4$ , respectively ( $\lambda_R = 0.1$ ). We have already mentioned the fact that all the above quantities become zero at  $T = T_{cr}$ . What becomes apparent in figs. 13, 14 is a critical behaviour which can be characterized by critical exponents. Following the notation of statistical mechanics, we parametrize the critical behaviour of  $\rho_0(T)$  and  $m_R^2(T)$  as follows:

$$\begin{aligned} \rho_0(T) &\propto (T_{cr}^2 - T^2)^{2\beta}, \\ m_R^2(T) &\propto (T^2 - T_{cr}^2)^{2\nu}. \end{aligned} \tag{5.4}$$

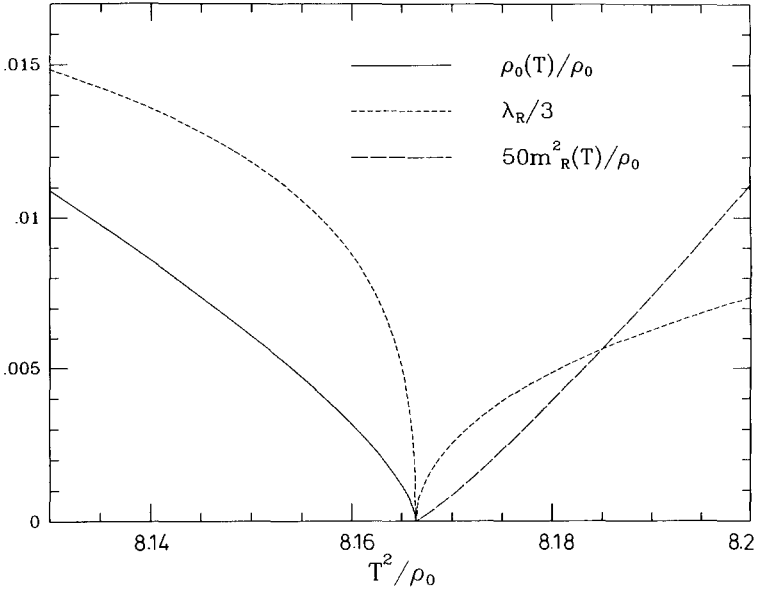


Fig. 13.  $\rho_0(T), \lambda_R(T), m_R^2(T)$  near  $T_{cr}$ , where the critical behaviour is apparent.  $N = 1, \lambda_R = 0.1, b = 3$ .

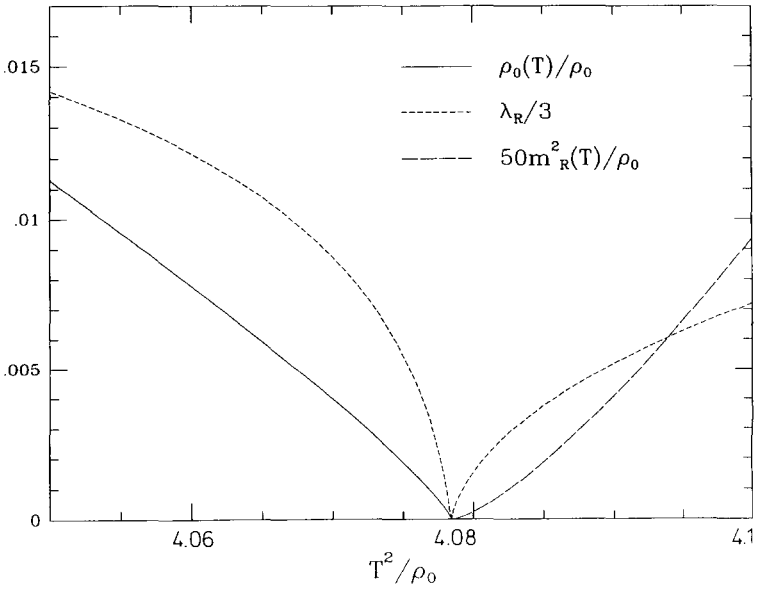


Fig. 14.  $\rho_0(T), \lambda_R(T), m_R^2(T)$  near  $T_{cr}$ , where the critical behaviour is apparent.  $N = 4, \lambda_R = 0.1, b = 3$ .

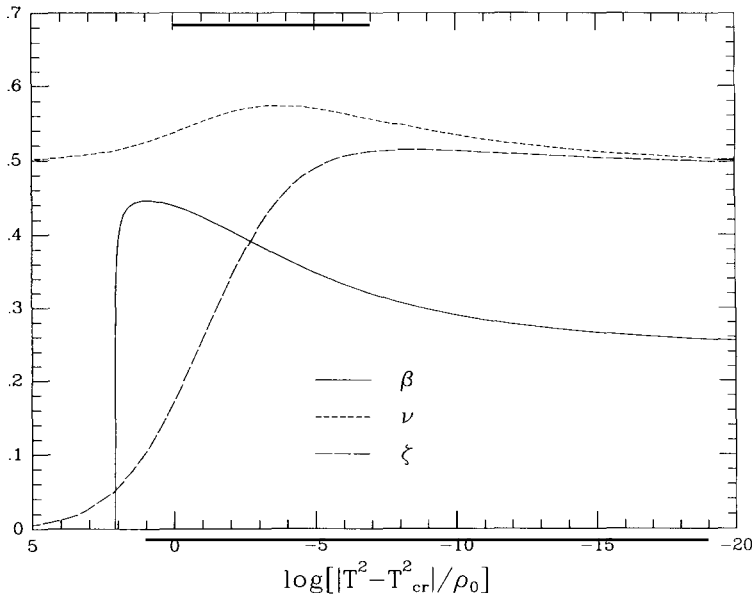


Fig. 15. The critical exponents as  $T_{cr}$  is approached. For  $T \rightarrow T_{cr}$  they become equal to the critical exponents of the zero temperature three-dimensional theory.  $N = 1, b = 3$ .

We also define a critical exponent  $\zeta$  for  $\lambda_R(T)$  in the symmetric regime:

$$\lambda_R(T) \propto (T^2 - T_{cr}^2)^\zeta. \tag{5.5}$$

These exponents are plotted as function of the logarithm of  $|T^2 - T_{cr}^2|$  in figs. 15 and 16 for  $N = 1$  and  $N = 4$ , respectively. (We should note at this point that, in the limit  $T \rightarrow T_{cr}$ , the above definition coincides with the more conventional one, which is given in terms of  $|T - T_{cr}|$ . We have used this parametrization for uniformity since everything in this section has been expressed in terms of  $T^2/\rho_0$ . The temperature dependent exponent  $2\beta$  is defined as the derivative of  $\ln \rho_0$  with respect to  $\ln |T^2 - T_{cr}^2|$ , and similarly for the other exponents.) We notice that in the limit  $T \rightarrow T_{cr}$  the critical exponents approach asymptotic values. These are independent of  $\lambda_R$  and therefore fall into universality classes determined only by  $N$ . They are equal to the critical exponents of the zero temperature three-dimensional theory. This fact can be understood by recalling that the evolution in the high temperature region is determined by an effective three dimensional theory (see the discussion in sect. 4), whose phase diagram (figs. 5 and 6) has a fixed point corresponding to the phase transition. For  $T \rightarrow T_{cr}$  the evolution of  $\rho_0(k, T), \lambda(k, T)$  in the high temperature region is given by a line in the phase diagram very close to the critical line. In this case  $\rho_0(k, T), \lambda(k, T)$  spend an arbitrarily long “time”  $t$  close to the fixed point and,

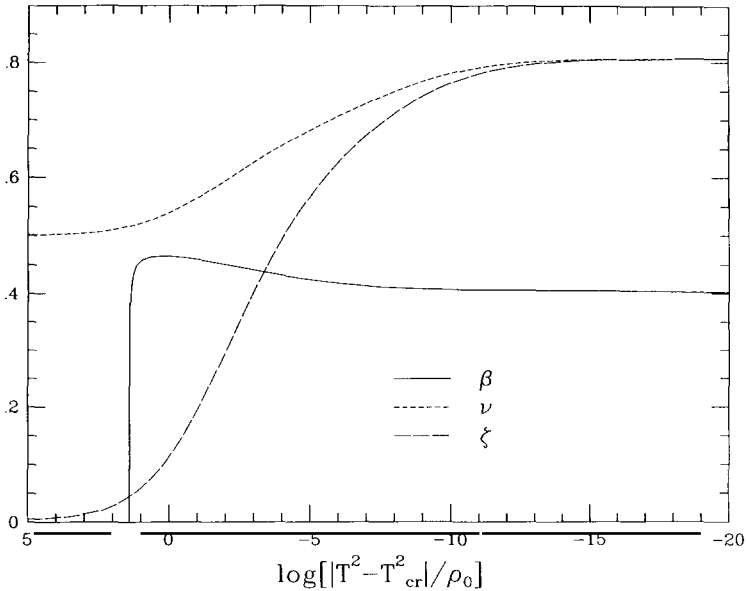


Fig. 16. The critical exponents as  $T_{cr}$  is approached. For  $T \rightarrow T_{cr}$  they become equal to the critical exponents of the zero temperature three-dimensional theory.  $N = 4, b = 3$ .

as a result, lose memory of their “initial values”  $\rho_0(T/\theta_2, T), \lambda(T/\theta_2, T)$ . The critical behaviour is determined solely by the fixed point, without any memory of the evolution in the zero temperature or threshold region.

We have now established the connection between the critical behaviour of the non zero temperature four-dimensional theory and the zero temperature three dimensional one. As a result we have a large amount of information, coming from detailed investigations in statistical field theory, which can serve as a check of our calculation. In table 4 we list the results of our calculation of  $\beta, \nu, \zeta$  for various  $N$ . The critical exponents  $\beta, \nu$  for the three-dimensional theory have been calculated by several methods:  $\epsilon$  expansion, summed perturbation theory in the symmetric phase in three dimensions,  $1/N$  expansion, lattice calculations. For comparison with our results we list in table 4 the most accurate values of  $\beta$  and  $\nu$  obtained by the previously mentioned methods. The agreement is good, even though we have neglected the wave function renormalization in this work. Preliminary results of a calculation which includes the wave function renormalization effects show even better agreement [14]. Another consistency check is provided by the scaling laws which give

$$\nu = 2\beta, \quad (5.6)$$

in the limit of zero wave function renormalization. The above relation is satisfied

TABLE 4

Critical exponents for various  $N$  ( $b = 3$ ). For comparison we have listed the results of various calculations of the exponents of the zero temperature three-dimensional theory as summarized in ref. [16]. (We have not included the errors quoted in ref. [16])

$N$	$\beta$		$\nu$	$\zeta$	
1	0.25	0.33 <sup>a)</sup> 0.31 <sup>b)</sup>	0.50	0.63 <sup>a,b)</sup>	0.50 = $\nu^c)$
3	0.37	0.37 <sup>a)</sup> 0.38 <sup>b)</sup>	0.75	0.71 <sup>a,b)</sup>	0.75 = $\nu^d)$
4	0.40		0.81		= $\nu^d)$
10	0.46	$\frac{1}{4}\gamma = 0.43^d)$	0.92	$\frac{1}{2}\gamma = 0.86^c)$	0.92 = $\nu^d)$
$\infty$		0.5 <sup>c)</sup>		1 <sup>c)</sup>	= $\nu^d)$

a) From  $\epsilon$ -expansion or summed perturbation theory in three dimensions.

b) From lattice calculations for the  $N$ -vector model.

c) From  $1/N$  expansion to order  $1/N^2$  [16]. The scaling laws give:  $\frac{1}{4}\gamma = \beta(1 - \frac{1}{2}\eta)/(1 + \eta)$ ,  $\frac{1}{2}\gamma = \nu(1 - \frac{1}{2}\eta)$ , where  $\eta$  is the wave function renormalization, which we have set to zero in this work.

d) From the finite value of  $\lambda_3/m$  at the critical point as given by summed perturbation theory, where  $\lambda_3$  is the renormalized three-dimensional coupling and  $m$  the renormalized mass [17,16].

by our numerical results to very good accuracy.

The critical behaviour of  $\lambda_R(T)$  is related to the resolution of the problem of the infrared divergences which cause the breakdown of the “naive” perturbative expansion in the limit  $T \rightarrow T_{cr}$  [1,3]. The infrared problem is manifest in the presence of higher order contributions to the effective potential which contain increasing powers of  $\lambda_R(T)T/k$ , where  $k$  is the effective infrared cutoff of the theory. If the evolution of  $\lambda(k, T)$  is omitted and  $\lambda_R(T)$  is approximated by its zero temperature value  $\lambda_R$ , these contributions diverge and the perturbative expansion breaks down. A similar situation appears for the zero temperature three-dimensional theory in the critical region [17]. In this case the problem results from an effective expansion in terms of the quantity  $u/[M^2 - M_{cr}^2]^{1/2}$ , where  $u$  is the bare three-dimensional quartic coupling and  $[M^2 - M_{cr}^2]^{1/2}$  is a measure of the distance from the point where the phase transition occurs as it is approached from the symmetric phase. The two situations can be seen to be of identical nature by simply remembering that the non-zero temperature four-dimensional coupling  $\lambda$  corresponds to an effective three-dimensional coupling  $\lambda T$  and that the effective infrared cutoff in the symmetric phase is equal to  $m_R(T)$ . In the three-dimensional case the problem has been resolved [17] by a reformulation of the calculation in terms of an effective parameter  $\lambda_3/m$ , where  $\lambda_3$  is the renormalized 1-PI four point function in three dimensions (the renormalized quartic coupling) and  $m$  the renormalized mass (equal to the inverse correlation length). It has been found [17,16] that the above quantity has an infrared stable fixed point in the critical region  $m \rightarrow 0$ . No infrared divergences arise within this approach. Their only residual effect is detected in the strong renormalization of  $\lambda_3$ . In our scheme the problem is formulated in terms of the effective dimensionless

TABLE 5

The asymptotic value of  $\lambda_R(T)T/m_R(T)$  in the limit  $T \rightarrow T_{cr}$  for various  $N$  ( $b = 3$ ). For comparison we have listed the values of  $\lambda_3/m$  at the critical point as given by summed perturbation theory, where  $\lambda_3$  is the renormalized three-dimensional coupling and  $m$  the renormalized mass [17,16]

$N$	1	3	4	10
$\lambda_R(T)T/m_R(T)$	6.8	5.5	4.8	3.7
$\lambda_3/m$	7.9	6.4		

parameters  $\tilde{\kappa}(k, T) = \rho_0(k, T)/kT$ ,  $\tilde{\lambda}(k, T) = \lambda(k, T)T/k$  (see eq. (4.11)), for which a fixed point corresponding to the phase transition is found. The critical behaviour is determined by this fixed point in the limit  $k \rightarrow 0$ . Everything remains finite in the vicinity of the critical temperature, and the only memory of the infrared divergences is reflected in the strong renormalization of  $\lambda_R(T)$  near  $T_{cr}$ . We conclude that the infrared problem disappears if formulated in terms of the appropriate renormalized quantities. When expressed in the correct language, it becomes simply a manifestation of the strong renormalization effects in the critical region. In order to compare with the three-dimensional results we have calculated the quantity  $\lambda_R(T)T/m_R(T)$  in the limit  $T \rightarrow T_{cr}$ . We find that it reaches an asymptotic value depending on  $N$ , which we list in table 5 for various  $N$ . For comparison we quote the results for the infrared fixed point of  $\frac{\lambda_3}{m}$  (for  $N = 1, 3$ ) as summarized in ref. [17,16]. Good agreement is observed. Moreover, the existence of the asymptotic value for  $\lambda_R(T)T/m_R(T)$  explains the equality of the critical exponents  $\nu$  and  $\zeta$  which is apparent in table 4.

Before concluding this section we would like to discuss an issue inherent in the formalism of the average potential. It concerns the dependence of the physical quantities on the scheme chosen in order to perform the averaging of fields over a volume  $k^{-d}$ . The averaging procedure results in an effective infrared cutoff  $\sim k$ . This is reflected in the modified propagator given by (2.4), (2.5). It is clear that the average potential  $U_k$  depends on the average parameters  $a$  and  $b$  appearing in (2.5). In the limit  $k \rightarrow 0$  the average potential approaches the effective potential [10] and, therefore, becomes independent of  $a$  and  $b$ . But the whole evolution of  $U_k$  starting from the "short distance values"  $\rho_0(k = \Lambda)$ ,  $\lambda(k = \Lambda)$  depends on the averaging scheme. The results of the present work concern the connection between the zero temperature ground state of the theory and the one for non-zero temperature. These are given by the effective potential ( $U_k$  in the limit  $k \rightarrow 0$ ) and should be independent of  $a$  and  $b$ . Even though the evolution carries some scheme dependence this should disappear when one calculates physical quantities such as the critical temperature or the critical exponents. Despite the above general arguments some scheme dependence is expected in our results. It comes from the approximations which are unavoidable in a practical calculation,

TABLE 6

$T_{\text{cr}}^2(N + 2)/\rho_0$  for various  $\lambda_R$  and  $N$ . Average parameter  $b = 4$ . To be compared to table 2, which has been generated with  $b = 3$

$N$	$\lambda_R = 0.01$	$\lambda_R = 0.1$	$\lambda_R = 1$
1	23.80	24.26	26.58
3	23.80	24.24	26.45
4	23.80	24.24	26.36
10	23.79	24.18	25.83

TABLE 7

$[m_R^2(T)/\lambda_R(T)(N + 2)T^2]^{-1}$  for  $T^2/\rho_0 = 10^6$  and various  $\lambda_R$ ,  $N$ . Average parameter  $b = 4$ . To be compared to table 3, which has been generated with  $b = 3$

$N$	$\lambda_R = 10^{-4}$	$\lambda_R = 0.01$	$\lambda_R = 0.1$
1	23.68	23.39	22.97
3	23.71	23.67	23.79
4	23.72	23.77	24.08
10	23.76	24.16	25.27

i.e. the consideration of the one loop average potential, the omission of the wave function renormalization, the truncation of the evolution equations, the uncertainties coming from the numerical solution. This is not a problem though. The  $b$  dependence of the results (in the family of parametrizations (2.6)) is a measure of the importance of the neglected terms and, therefore, of the accuracy of the calculation. We have performed the numerical solution of the evolution equations also for an average parameter  $b = 4$ , in order to compare with the results presented up till now, which were obtained for  $b = 3$ . In tables 6 and 7 we list the values of  $T_{\text{cr}}^2(N + 2)/\rho_0$  and  $[m_R^2(T)/\lambda_R(T)(N + 2)T^2]^{-1}$ , respectively, for various  $N$  and  $\lambda_R$  and for  $b = 4$ . These tables can be directly compared to tables 2 and 3, respectively. The numerical solution of the evolution equations involves larger uncertainties for  $b = 4$ . The oscillatory behaviour of the integrals  $L_n^4(\omega, T)$  in the threshold region is more pronounced and harder to reproduce by a numerical fit. As a result the 1% shift observed between tables 2, 3 and 6, 7 can be considered as a measure of the total uncertainties induced by the various analytic approximations as well as the limitations of the numerical solution. We postpone the discussion of the scheme dependence of the critical exponents for another publication which will include the wave function renormalization effects [14].

## 6. Approximate analytic results

In this section we derive analytic results for the critical temperature, the high and low temperature behaviour as well as for the critical exponents for  $T$  near  $T_{\text{cr}}$ , from approximate solutions of the evolution equations. We assume a sufficiently small value of the quartic coupling  $\lambda_{\text{R}}$ . As described at the end of sect. 4 we start from the physical zero temperature couplings at  $k = 0$ , use the four-dimensional evolution equations to solve for the relevant quantities  $\kappa$  and  $\lambda$  at the scale  $k_{\text{T}} = T/\theta_2 = 4l_1^3/l_1^4 T$ , apply the threshold correction for  $\kappa$  in order to obtain the initial values for the three-dimensional running at  $k = k_{\text{T}}$ , and finally follow the three-dimensional evolution equations for  $k \rightarrow 0$ . This procedure gives the effective physical couplings at non-vanishing temperature.

For small  $\lambda_{\text{R}}$  we approximate for the four-dimensional running

$$\begin{aligned} \frac{d\kappa}{dt} &= -2\kappa + (N+2)a_4, \\ a_4 &= \frac{l_1^4}{16\pi^2}. \end{aligned} \quad (6.1)$$

This gives:

$$\kappa(k_{\text{T}}) = \frac{N+2}{2}a_4 + \frac{\rho_0}{k_{\text{T}}^2}. \quad (6.2)$$

The threshold correction

$$\delta\kappa = \frac{N+2}{2}\Delta \quad (6.3)$$

results in an effective shift  $a_4 \rightarrow a_4 + \Delta$  in (6.2). In consequence, the initial values for the three-dimensional running read:

$$\tilde{\kappa}(k_{\text{T}}, T) = 2(N+2)l_1^3 \left( \frac{1}{16\pi^2} + \frac{\Delta}{l_1^4} \right) + \frac{l_1^4}{4l_1^3} \frac{\rho_0}{T^2}, \quad (6.4)$$

$$\tilde{\lambda}(k_{\text{T}}, T) = \frac{l_1^4}{4l_1^3} \lambda(k_{\text{T}}). \quad (6.5)$$

Here  $\lambda(k_{\text{T}})$  accounts for the logarithmic four-dimensional running of  $\lambda(k)$ . We observe that  $\tilde{\lambda}(k_{\text{T}}, T)\tilde{\kappa}(k_{\text{T}}, T) = \lambda(k_{\text{T}}, T)\kappa(k_{\text{T}}, T) \ll 1$  for small  $\lambda_{\text{R}}$  and  $T^2 \gg \frac{1}{16}\lambda_{\text{R}}\rho_0$ . For  $N > 1$  one can use analogous formulae also for  $T^2 \ll \frac{1}{16}\lambda_{\text{R}}\rho_0$  by replacing everywhere the factor  $N+2$  by  $N-1$ . Only the  $N-1$  Goldstone bosons contribute effectively to the running for  $\lambda\kappa \gg 1$ . For the three-dimensional running we consider first the region where  $\tilde{\lambda}\tilde{\kappa}$  remains much smaller than one.

Then we can approximate

$$\begin{aligned} \frac{d\tilde{\kappa}}{dt} &= -\tilde{\kappa} + (N + 2)a_3, \\ a_3 &= \frac{l_1^3}{4\pi^2} \end{aligned} \tag{6.6}$$

and find the solution

$$\tilde{\kappa}(k, T) = (N + 2)a_3 + \frac{k_T}{k} \{ \tilde{\kappa}(k_T, T) - (N + 2)a_3 \}. \tag{6.7}$$

*Critical temperature.* The critical temperature is determined by the requirement that the pair  $(\tilde{\kappa}(k_T, T), \tilde{\lambda}(k_T, T))$  as given by (6.4), (6.5) corresponds to a point on the critical line in the phase diagram of figs. 5 and 6. For small  $\lambda_R$  this is equivalent to the ultraviolet stable fixed point for  $\tilde{\kappa}$  following from (6.6), namely:

$$\tilde{\kappa} = (N + 2)a_3. \tag{6.8}$$

Inserting (6.8) into (6.4) for  $T = T_{cr}$  yields:

$$R = \frac{T_{cr}^2(N + 2)}{\bar{\rho}_0} = \frac{l_1^4}{(l_1^3)^2} \left( \frac{1}{2\pi^2} - \frac{8\Delta}{l_1^4} \right)^{-1} = 23.94. \tag{6.9}$$

Here the numerical value is given for an average parameter  $b = 3, l_1^4 = 0.7205, l_1^3 = 0.8333, \Delta = 6.59 \times 10^{-4}$ . It is remarkable how close this value comes to the “naive” perturbative result  $T_{cr}^2 = 24\rho_0/(N + 2)$  [2]. Without the threshold correction ( $\Delta = 0$ )  $R$  would be 20.48, which is still in good qualitative agreement with the perturbative result. Both with and without the threshold correction the analytic result agrees well with the corresponding numerical values ( $R = 24.05 - 24.02$  and  $R = 20.56 - 20.54$  for  $\lambda_R = 0.01, b = 3$  and  $N = 1 - 10$ ). We infer from the phase diagrams (figs. 5,6) that for increasing  $\tilde{\lambda}(k_T, T)$  the critical value of  $\tilde{\kappa}(k_T, T)$  decreases. The critical temperature therefore increases.

*High temperature behaviour.* For  $T$  larger than  $T_{cr}$  the global  $O(N)$  symmetry remains unbroken (symmetric phase). The product  $\tilde{\lambda}\tilde{\kappa}$  remains small for small  $\lambda_R$ . The minimum of  $U_k$  runs to the origin at some scale  $k_s > 0$

$$\tilde{\kappa}(k_s, T) = 0. \tag{6.10}$$

We write

$$k_s = K \left( \frac{\rho_0}{T^2} \right) T \tag{6.11}$$

and determine  $K$  from (6.7)

$$K \left( \frac{\rho_0}{T^2} \right) = \frac{l_1^3}{l_1^4} \left( 2 - \frac{32\pi^2\Delta}{l_1^4} - \frac{4\pi^2 l_1^4}{(l_1^3)^2(N + 2)} \frac{\rho_0}{T^2} \right). \tag{6.12}$$

For large  $T$  the function  $K$  approaches a constant and  $k_s \simeq \frac{1}{2}k_T$ . For small  $\lambda_R$  there is therefore only very little running of  $\lambda(k, T)$  between  $k_T$  and  $k_s$ . Thus

$$\lambda(k_s, T) = \lambda(k_T, T). \quad (6.13)$$

At scales  $k < k_s$  we have to continue the evolution equations in the symmetric regime. In particular, the mass term  $m^2(k, T) = U'_k(0, T)$  obeys

$$\frac{dm^2}{dk} = -\frac{N+2}{4\pi^2} l_1^3 s_1^3 \left( \frac{m^2}{k^2} \right) \lambda T, \quad (6.14)$$

with  $m^2(k_s) = 0$ . The physical mass obtains as  $m_R^2(T) = m^2(k \rightarrow 0, T)$ . By pure dimensional arguments one finds  $m_R^2(T) \sim T^2$ , since in the high temperature limit  $k_s \simeq (2l_1^3/l_1^4)T$ ,  $\lambda(k_T, T) \simeq \lambda_R$ . For an approximate solution of (6.14) we neglect the running of  $\lambda$  and approximate  $s_1^3 = 1$ . In this way we obtain:

$$m^2(k, T) = [(N+2)/4\pi^2] l_1^3 \lambda_R T (k_s - k). \quad (6.15)$$

This approximation is justified for  $k \gg \lambda_R T / 4\pi^2$  where the three-dimensional running of  $\lambda(k, T)$  can be neglected and  $k^2 \gg [(N+2)/2\pi^2] \lambda_R T^2$  where  $m^2(k, T)/k^2$  remains small. Since the modifications of the running for very small  $k$  give only corrections which vanish for  $\lambda_R \rightarrow 0$  we obtain the leading order result for  $m_R^2(T)$  by extrapolating (6.15) to  $k \rightarrow 0$ :

$$\frac{m_R^2(T)}{(N+2)\lambda_R(T)T^2} = \frac{l_1^3}{4\pi^2} K\left(\frac{\rho_0}{T^2}\right) \rightarrow \frac{1}{R}. \quad (6.16)$$

The last result indicates the high temperature limit where corrections  $\sim \rho_0/T^2$  are neglected. In lowest order in  $\lambda_R$  we recover the perturbative relation with the critical temperature

$$\lim_{T \rightarrow \infty} m_R^2(T) = \frac{\lambda_R(T)\rho_0}{T_{cr}^2} T^2. \quad (6.17)$$

Again, our numerical results coincide well with the analytic relation (6.16).

The good agreement between our method and high temperature perturbation theory for  $T \gg T_{cr}$  should be of no surprise, since this is the temperature regime where the latter is expected to be valid. It may be more puzzling that high temperature perturbation theory leads to a good estimate for the critical temperature, although we have seen that physics near  $T_{cr}$  is quite different from the naive perturbative results and, in particular, not characterized by a small parameter  $\lambda$ . The reason is that  $T_{cr}$  can be determined from the behaviour of the critical line in the phase diagram (figs. 5, 6) near  $\tilde{\lambda} = 0$ . It does not need the understanding of the more complicated physics near the fixed point which characterizes the behaviour at  $T = T_{cr}$ . In turn, the critical line near  $\tilde{\lambda} = 0$  can be obtained in perturbation theory if the quartic coupling (for  $T = 0$ ) is small.

*Low temperature behaviour.* Let us first consider the region

$$\frac{1}{16}\lambda_R\rho_0 \ll T^2 \ll T_{cr}^2 \quad (6.18)$$

where we can use (6.4) as initial value and (6.7) for the three-dimensional running. Inserting the definition of  $\tilde{\kappa}(k, T)$  in terms of  $\rho_0(k, T)$  (4.11) one finds:

$$\rho_0(T) = \rho_0 - \frac{N + 2}{R} T^2. \tag{6.19}$$

This linear behaviour agrees qualitatively with figs. 11 and 12, but we note that the true values lie actually somewhat above the straight line (6.19). Indeed, there is always a region of the running for small  $k$  where  $\tilde{\lambda}\tilde{\kappa} > 1$  such that  $\rho_0(k, T)$  decreases slower than implied by (6.7). This explains the small difference. Furthermore, the slope  $-d\rho_0(T)/dT^2$  is smaller than  $(N + 2)/R$  at the origin. In fact, for  $N > 1$  and  $T^2 \ll \frac{1}{16}\lambda_R\rho_0$  the above formulae should be used with  $N - 1$  replacing  $N + 2$ . This gives the correct slope in the immediate vicinity of  $T = 0$ . We emphasize, however, that the region in  $T^2/\rho_0$  where the behaviour is purely dominated by the  $N - 1$  Goldstone bosons is very small, especially for small  $\lambda_R$ . Denoting the mass of the radial excitation (“ $\sigma$ -field”) in the spontaneously broken phase by  $M^2 = 2\lambda_R\rho_0$  we find that the radial mode becomes important for  $T^2 > \frac{1}{32}M^2$ . This remark may be relevant for the treatment of the non-zero temperature behaviour of QCD by means of chiral perturbation theory.

*Critical exponents.* For the discussion of the behaviour near the critical temperature we cannot use the approximation (6.6), since  $\tilde{\lambda}\tilde{\kappa}$  is not small near the fixed point characterizing the phase transition ( $\tilde{\lambda}_{fp}\tilde{\kappa}_{fp} = 0.45$  for  $N = 1$ ,  $\tilde{\lambda}_{fp}\tilde{\kappa}_{fp} = 0.70$  for  $N = 4$ ). We therefore start with the full high temperature evolution equation for  $\rho_0(k, T)$  (4.12)

$$\frac{d\rho_0}{dt} = \frac{l_1^3}{4\pi^2} \{N - 1 + 3s_1^3(2\tilde{\lambda}\tilde{\kappa})\}. \tag{6.20}$$

For  $T = T_{cr}$  there is a critical trajectory  $\rho_0^{cr}(k, T)$  which corresponds to the critical line separating the two phases of the diagrams 5 and 6. Its behaviour for  $k \rightarrow 0$  is characterized by the fixed point  $\tilde{\kappa} = \tilde{\kappa}_{fp}$ ,

$$\rho_0^{cr}(k, T) = \tilde{\kappa}_{fp} T_{cr} k. \tag{6.21}$$

We are interested in temperatures in the vicinity of  $T_{cr}$ , i.e.  $|T - T_{cr}| \ll T_{cr}$ , where the relevant trajectories are near the critical line. We parametrize

$$\rho_0(k, T) = \rho_0^{cr}(k, T) + \delta\rho_0(k, T) \tag{6.22}$$

and linearize the evolution equations as long as  $|\delta\rho_0(k, T)| \ll \rho_0^{cr}(k, T)$ , using (4.12) and  $(d/dy)s_1^3(y) = -(l_2^3/l_1^3)s_2^3(y)$

$$\frac{d(\delta\rho_0)}{dt} = \tau \delta\rho_0, \tag{6.23}$$

where

$$\tau(\tilde{\lambda}\tilde{\kappa}) = \frac{\partial}{\partial(\delta\rho_0)} \frac{d}{dt}(\delta\rho_0) = 1 + \frac{\partial}{\partial\tilde{\kappa}} \frac{d\tilde{\kappa}}{dt} = -\frac{3l_2^3}{2\pi^2} \tilde{\lambda}s_2^3(2\tilde{\lambda}\tilde{\kappa}). \tag{6.24}$$

As long as  $\tilde{\lambda}$  and  $\tilde{\kappa}$  are running near the critical line the quantity  $\tau$  depends on  $k$ . We can define an average value

$$\bar{\tau}(k) = \left[ \int_{\ln k}^{\ln k_T} \tau(t) dt \right] / \left[ \ln \frac{k_T}{k} \right] \tag{6.25}$$

such that

$$\delta \rho_0(k, T) = \delta \rho_0(k_T, T) \left( \frac{k}{k_T} \right)^{\bar{\tau}(k)}. \tag{6.26}$$

Very near the critical temperature, however, the relevant trajectory remains in the immediate vicinity of the fixed point  $(\tilde{\kappa}_{fp}, \tilde{\lambda}_{fp})$  for most of the running. In the limit  $T \rightarrow T_{cr}$  the average reaches the asymptotic limit

$$\lim_{k \rightarrow 0} \bar{\tau}(k) = \tau_{fp} = -\frac{3l_2^3}{2\pi^2} \tilde{\lambda}_{fp} \delta_2^3 (2\tilde{\lambda}_{fp} \tilde{\kappa}_{fp}). \tag{6.27}$$

The asymptotic evolution of  $\delta \rho_0$  is characterized by a constant anomalous dimension  $\tau_{fp}$ . With  $b = 3$  we find  $\tau_{fp} = -0.667$  for  $N = 1$  and  $\tau_{fp} = -0.193$  for  $N = 4$ . The initial value  $\delta \rho_0(k_T)$  can be expressed in terms of  $T_{cr} - T$  from (6.4)

$$\begin{aligned} \delta \rho_0(k_T, T) &= \frac{4l_1^3}{l_1^4} T_{cr}^2 \delta \tilde{\kappa}(k_T, T) \\ &= \frac{4l_1^3}{l_1^4} T_{cr}^2 \frac{\partial \tilde{\kappa}}{\partial T}(k_T, T_{cr}) (T - T_{cr}) \\ &= 2 \frac{\rho_0}{T_{cr}} (T_{cr} - T). \end{aligned} \tag{6.28}$$

Since  $\bar{\tau} < 0$ ,  $|\delta \rho_0(k, T)|$  increases for decreasing  $k$ . For any non-zero  $\delta \rho_0(k_T, T)$  there will be some scale  $k_F$  where  $|\delta \rho_0(k_F, T)| = c \rho_0^{cr}(k_F, T)$  with  $c$  some constant of order unity which we take smaller than one. For  $k < k_F$  the linear approximation (6.24) for the running of  $\delta \rho_0$  breaks down and the trajectory goes away from the fixed point. Depending on  $\delta \rho_0$  being positive or negative one ends in the spontaneously broken or symmetric phase. In the spontaneously broken phase  $\rho_0$  essentially stops running somewhat below the scale  $k_F$  so that its value for  $k \rightarrow 0$  is proportional to  $\delta \rho_0(k_F, T)$

$$\rho_0(T) = \alpha(c) \delta \rho_0(k_F, T). \tag{6.29}$$

For  $c = 0.1$  we find numerically  $\alpha(c) = 0.2$  for  $N = 1$ , and  $\alpha(c) = 0.5$  for  $N = 4$ . The scale  $k_F$  is determined by (6.21), (6.26) and (6.28) (where  $\bar{\tau}$  stands for  $\bar{\tau}(k_F)$ ). From

$$\delta \rho_0(k_T, T) \left( \frac{k_F}{k_T} \right)^{\bar{\tau}} = c \tilde{\kappa}_{fp} T_{cr} k_F, \tag{6.30}$$

TABLE 8

Critical exponents for various  $N$  as calculated from the approximate analytic expressions of sect. 6 ( $b = 3$ ). To be compared to table 4

$N$	$\beta$	$\nu$	$\zeta$
1	0.30	0.60	0.60
3	0.40	0.80	0.80
4	0.42	0.84	0.84
10	0.47	0.93	0.93

we find

$$\frac{k_F}{k_T} = f (T_{cr} - T)^{1/(1-\bar{\tau})}, \tag{6.31}$$

$$f = \left( \frac{l_1^4 \rho_0}{2l_1^3 c \tilde{\kappa}_{fp} T_{cr}^3} \right)^{1/(1-\bar{\tau})}. \tag{6.32}$$

This yields finally

$$\begin{aligned} \rho_0(T) &= B^2 (T_{cr} - T)^{1/(1-\bar{\tau})}, \\ B^2 &= \frac{2\alpha(c) f^{\bar{\tau}} \rho_0}{T_{cr}}, \end{aligned} \tag{6.33}$$

where  $\bar{\tau}$  may now be considered as a function of  $T_{cr} - T$  by using (6.31), (6.32). We note again that the asymptotic value of the critical exponent  $\beta = 1/2(1 - \tau_{fp})$  is universal for all three-dimensional  $O(N)$ -symmetric scalar theories with given  $N$ . The values of  $\beta$  obtained by using eq. (6.27) are listed in table 8 and are in good agreement with the numerical results (compare table 4). The proportionality factor  $B^2$  is not universal for all three-dimensional theories. It reflects the particular embedding of the effective three-dimensional theory for momenta  $q^2 \ll T^2$  in the full relativistic four-dimensional scalar model. In this sense it is a property of the four-dimensional theory. Numerically we find in units of  $\rho_0$ :  $B^2 = 0.037$  for  $N = 1$ , and  $B^2 = 0.45$  for  $N = 4$ . These values are very sensitive to the precise value of the critical exponents. Therefore, they are afflicted with rather large numerical uncertainties. The above numerical results are consistent with the analytic expressions (6.32), (6.33).

In the symmetric phase the linear approximation for the running of  $\delta \rho_0$  breaks again down for  $|\delta \rho_0(k_F, T)| = c \rho_0^{cr}(k_F, T)$ . The minimum of the potential runs to the origin at  $k_s \sim k_F$  and from there on one continues the running in the symmetric regime. Since  $\tilde{\lambda}(k_F, T) \simeq \tilde{\lambda}_{fp}$  the scale  $k_F$  (or similar for  $k_s$ ) is the only scale present for the running with  $k < k_F$ . One concludes from dimensional arguments that

$$m_R^2(T) = \tilde{\alpha}(c) k_F^2. \tag{6.34}$$

This leads again to a behaviour with a critical exponent

$$m_{\text{R}}^2(T) = N_+^2 (T - T_{\text{cr}})^{2/(1-\bar{\tau})},$$

$$N_+^2 = \left( \frac{4l_1^3}{l_1^4} \right)^2 \tilde{\alpha}(c) f^2 T_{\text{cr}}^2. \quad (6.35)$$

The critical exponent  $\nu = 1/(1 - \tau_{\text{fp}})$  is universal and we recover the relation  $\nu = 2\beta$ , as appropriate when neglecting the wave function renormalization. It also follows from dimensional arguments that  $\lambda_{\text{R}}(T)T$  must be proportional to  $k_{\text{F}}$ . This gives the scaling relation

$$\lim_{T \rightarrow T_{\text{cr}}} \frac{\lambda_{\text{R}}(T)T}{m_{\text{R}}(T)} = \text{const.} \quad (6.36)$$

which leads to the relation  $\zeta = \nu$ .

## 7. Conclusions

We have employed a new method in order to compute the temperature dependent effective potential for the  $N$ -component  $\phi^4$  theory. This method describes properly the four-dimensional running of couplings at scales  $k$  large compared to  $T$  and the effective three-dimensional running for  $k \ll T$ . The infrared behaviour of the theory is fully understood and no divergences appear even at the critical temperature. The high temperature phase transition is second order. No ‘‘cubic term’’ appears in the potential. At the critical temperature the quartic coupling vanishes and the lowest interaction is a (universal)  $\phi^6$  coupling (up to small corrections coming from the wave function renormalization). Near the critical temperature the mass and the quartic coupling behave  $\sim (T - T_{\text{cr}})^\nu$ , where  $\nu$  is the critical exponent of the three dimensional theory. Nevertheless, high temperature ‘‘naive’’ perturbation theory gives reliable estimates for the range  $T \gg T_{\text{cr}}$  and for the determination of  $T_{\text{cr}}$  (if  $\lambda$  is sufficiently small).

Our results are based on a one loop calculation which goes beyond the lowest order perturbation theory (even with the inclusion of ‘‘daisy’’ diagrams). In high temperature ‘‘naive’’ perturbation theory the expansion parameter is  $\lambda T/m(T)$  and diverges for  $m(T) \rightarrow 0$ . In our case it is replaced by a running coupling  $\lambda(k, T)T/k$ . This ratio remains finite for  $k \rightarrow 0$  at the critical temperature. For  $T = T_{\text{cr}}$  it actually runs to a fixed point  $\tilde{\lambda}_{\text{fp}}$ . There are no infrared divergences and the relevant parameter does not grow as the critical temperature is approached. On the other hand  $\tilde{\lambda}_{\text{fp}}$  is not particularly small and an expansion in powers of  $\tilde{\lambda} = \lambda(k, T)T/k$  does not converge rapidly. It may therefore seem surprising that our one loop results give such a good description of the phase transition, including correct values for the critical exponents. We should emphasize at this place that the loop expansion in our case is not a power series

in  $\tilde{\lambda}$ . Already the one loop calculation leads to non-trivial functions of  $\tilde{\lambda}$ . This results from the threshold effects which take the relevant mass terms at a given scale  $k$  properly into account. In addition, we can deal with the fact that the average potential is not purely quartic and include, for example, the effective  $\phi^6$  term [14]. Our picture of an effective action for averages of fields, where we always work around the minimum of the  $k$ -dependent potential with appropriate masses for all fluctuations, seems to include all relevant physics. We believe that it actually takes into account in one loop order many of the effects which would only appear in higher loop order in more standard formulations of perturbation theory. More formally the quadratic term in the functional integration is enhanced by the constraint, thus improving the validity of the saddle point expansion. Only modes with momenta between  $k$  and the ultraviolet cutoff  $\Lambda$  are effectively integrated. Our calculation can be reformulated [10] as a “block spin” approach [18,19]. At every step the ultraviolet cutoff can then be taken as a function of  $k$ , i.e.  $\Lambda = \hat{c}k$  [10], with  $\hat{c}$  some constant larger than one. (Since the ultraviolet cutoff is exponential in our case we actually work effectively with moderate values of  $\hat{c}$ , say  $\hat{c}$  around three.) It has been proven rigorously [10] that the one loop approximation becomes exact in the limit  $\hat{c} \rightarrow 1$ . In this limit the evolution equations are of the type of those discussed in reference [18,20] and coincide with them in special limits. This gives additional motivation to believe that our one loop result is much more reliable than an expansion in powers of  $\tilde{\lambda}$ .

We finally should comment on the possible extension of our results to the standard model. The inclusion of chiral fermions does not pose any particular problems in our formulation [21]. The average action has also been formulated for gauge theories [22] but detailed calculations are available so far only for the abelian case. Near the phase transition one expects strong effects from the three-dimensional running of the gauge coupling. Before they are properly taken into account a statement on the order and the details of the high temperature phase transition in the standard model seems premature.

We would like to thank S. Bornholdt, F. Borzumati and M. Drees for their help with the numerics. After this work was completed we became aware of the preprint [23] in which the importance of the evolution of  $\lambda$  is pointed out. For some recent studies of higher order perturbative contributions to the effective potential near the phase transition see ref. [24]. The four-dimensional  $\phi^4$  theory at non-zero temperature has been studied on the lattice [25]. The phase transition was found to be of the second order and the scaling behaviour was in good agreement with that of the three-dimensional theory at zero temperature.

**References**

- [1] D.A. Kirzhnits and A.D. Linde, Phys. Lett. B42 (1972) 471; Ann. Phys. (NY) 101 (1976) 195
- [2] L. Dolan and R. Jackiw, Phys. Rev. D9 (1974) 3320
- [3] S. Weinberg, Phys. Rev. D9 (1974) 3357
- [4] V.A. Kuzmin, V.A. Rubakov and M.E. Shaposhnikov, Phys. Lett. B155 (1985) 36;  
M.E. Shaposhnikov, Nucl. Phys. B287 (1987) 757; B299 (1988) 797;  
A.I. Bochkarev, S.Y. Khlebnikov and M.E. Shaposhnikov, Nucl. Phys. B329 (1990) 493
- [5] L. McLerran, Phys. Lett. B62 (1989) 1075;  
A.G. Cohen, D.B. Kaplan and A.E. Nelson, Phys. Lett. B245 (1990) 561; Nucl. Phys. B349 (1991) 727;  
N. Turok and J. Zadrozny, Phys. Rev. Lett. 65 (1990) 2331
- [6] A.D. Linde, Phys. Lett. B96 (1980) 289
- [7] S. Coleman and E. Weinberg, Phys. Rev. D7 (1973) 1888
- [8] A.I. Bochkarev and M.E. Shaposhnikov, Mod. Phys. Lett. A2 (1987) 417;  
A.I. Bochkarev, S.V. Kuzmin and M.E. Shaposhnikov, Phys. Lett. B244 (1990) 257;  
N. Turok and J. Zadrozny, Nucl. Phys. B369 (1992) 729;  
G. Anderson and L.J. Hall, Phys. Rev. D45 (1992) 2685;  
M. Dine, P. Huet and R. Singleton, Nucl. Phys. B375 (1992) 625;  
M.E. Shaposhnikov, Phys. Lett. B277 (1992) 324;  
M. Dine, R.G. Leigh, P. Huet, A.D. Linde and D.A. Linde, Phys. Rev. D46 (1992) 550
- [9] K. Takahashi, Z. Phys. C26 (1985) 601;  
M.E. Carrington, Phys. Rev. D45 (1992) 2933;  
A. Linde, preprint SU-ITP-92-18
- [10] C. Wetterich, Nucl. Phys. B352 (1991) 529
- [11] C. Wetterich, preprint DESY-91-088
- [12] A. Ringwald and C. Wetterich, Nucl. Phys. B334 (1990) 506
- [13] N. Tetradis and C. Wetterich, Nucl. Phys. B383 (1992) 197
- [14] N. Tetradis and C. Wetterich, in preparation
- [15] J. Kapusta, Finite temperature field theory (Cambridge Univ. Press, Cambridge, 1989)
- [16] J. Zinn-Justin, Quantum field theory and critical phenomena (Oxford Science Publications, 1989)
- [17] G. Parisi, J. Stat. Phys. 23 (1980) 49; Statistical field theory, (Addison-Wesley, New York, 1988)
- [18] K.G. Wilson, Phys. Rev. B4 (1971) 3174, 3184 ;  
K.G. Wilson and I.G. Kogut, Phys. Rep. 12 (1974) 75
- [19] L.P. Kadanoff, Physics 2 (1966) 263
- [20] J. Polchinski, Nucl. Phys. B231 (1984) 269;  
S.K. Ma, Modern theory of critical phenomena (Benjamin-Cummings, Menlo Park, CA, 1976)
- [21] C. Wetterich, Z. Phys. C48 (1990) 693
- [22] M. Reuter and C. Wetterich, preprint DESY-92-037
- [23] D. O'Connor, C.R. Stephens and F. Freire, preprint DIAS-STP-92-02
- [24] V. Jain, preprint MPI-PH-92-41;  
J.R. Espinosa, M. Quiros and F. Zwirner, Phys. Lett. B291 (1992) 115
- [25] K. Jansen and P. Seufferling, Nucl. Phys. B343 (1990) 507